[AMERICAN JOURNAL OF SCIENCE, VOL. 294, APRIL, 1994, P. 485–528]

MAGNETIZATION AND GEOCHEMISTRY OF GREIGITE-BEARING CRETACEOUS STRATA, NORTH SLOPE BASIN, ALASKA

RICHARD L. REYNOLDS, MICHELE L. TUTTLE, CYNTHIA A. RICE, NEIL S. FISHMAN, JOHN A. KARACHEWSKI,* and DAVID M. SHERMAN**
U.S. Geological Survey, Box 25046, Mail Stop 964
Denver, Colorado 80225

ABSTRACT. Postdepositional greigite (Fe_3S_4; ferrimagnetic thiospinel) is of interest to sedimentary geochemists, because it reflects important reactions during diagenesis and to paleomagnetists because it can obscure a detrital paleomagnetic record. The presence, distribution, and origin of greigite are best understood through combined magnetic and geochemical studies. Such studies of greigite-bearing Upper Cretaceous siliciclastic beds from the Simpson Peninsula, North Slope, Alaska, reveal relations among sulfur species and magnetic properties, and they illustrate the use of geochemical analysis to constrain the age of secondary magnetization carried by greigite. Greigite is ubiquitous in marine mudstone of the Seabee Formation, and it dominates the magnetic properties of the Seabee (magnetic susceptibility [MS]: 5.9×10^{-4} volume SI; magnitude of natural remanent magnetization [NRM]: 6.6×10^{-2} amperes/meter [A/m]; averages of 22 specimens in which greigite is the only magnetic mineral). The Seabee rocks fill an ancient submarine canyon cut into marine, transitional, and nonmarine sandstone, siltstone, and mudstone beds of the undifferentiated Ninuluk and Seabee Formations. In these sandstone and siltstone beds, some of which contain biodegraded oil, greigite occurs sporadically but is locally concentrated to yield high values of MS (5×10^{-3} vol. SI) and NRM magnitude (0.5 A/m). Samples that contain detrital iron-titanium oxides, principally titanohematite, as the only magnetic minerals have lower values of MS and NRM magnitude.

Different geochemical signatures in the Seabee Formation and undifferentiated Ninuluk and Seabee rocks indicate different origins of their greigite and associated iron disulfide minerals. In the Seabee, greigite and pyrite formed during early diagenesis via bacterial sulfate reduction utilizing indigenous sulfate and organic carbon. Evidence for early diagenetic iron sulfide includes (1) negative $\delta^{34}S$ values (typically between −22 and −30 permil) of acid-volatile sulfur (sulfur in greigite) and disulfide sulfur; and (2) the common presence of greigite and framboidal pyrite in detrital plant fragments. Ratios of total reduced mineral sulfur to organic carbon (S/C) indicate low contents of sulfur relative to those of normal marine sediments. In the undifferentiated Ninuluk and Seabee rocks, reactions that involved epigenetic sulfur produced greigite, pyrite, and rare marcasite that cement and surround early diagenetic pyrite. In many of these beds, S/C ratios are high relative to normal marine sediments. The epigenetic

* Present address: 1455 Balhan Drive, Concord, California 94521.
** Present address: Pacific Northwest Laboratory, P.O. Box 999, Richland, Washington 99352.

sulfur may have been derived from (1) sulfate-bearing Paleozoic units in deeper parts of the North Slope basin to the south, perhaps during much of the Tertiary to the present; or (2) the canyon-fill Seabee during compaction of the marine mud. Bacterial sulfate reduction (BSR) in a sulfate-limited environment is indicated from many $\delta^{34}S$ values (> +22 permil) that exceed the expected values for sulfate minerals (formed from seawater sulfate) in any unit in the basin. Organic substances that supported such BSR in the undifferentiated Ninuluk and Seabee rocks may have been derived from hydrocarbons.

INTRODUCTION

The alteration of sediments and sedimentary rocks under geochemically reducing conditions can change rock-magnetic properties (Henshaw and Merrill, 1980; Karlin and Levi, 1985; Karlin, 1990a, b; Canfield and Berner, 1987; Leslie and others, 1990; Leslie, Lund, and Hammond, 1990; Channell and Hawthorne, 1990). In particular the magnetization may be diminished when pyrite (FeS_2) replaces preexisting magnetic oxide minerals (Karlin and Levi, 1985; Canfield and Berner, 1987; Channell and Hawthorne, 1990; Goldhaber and Reynolds, 1991), or the original directions and magnitudes of magnetization may be changed by the authigenic growth of ferrimagnetic pyrrhotite (Fe_7S_8) or greigite (Fe_3S_4) (Clark, 1983; Reynolds and others, 1990; Reynolds, Fishman, and Hudson, 1991).

With regard to greigite, we still have much to learn about its origins, its occurrences, its geochemical and magnetic stabilities, and even its fundamental magnetic properties and crystal chemistry. Moreover, some standard bulk-sediment magnetic tests used routinely to distinguish among common magnetic minerals, such as magnetite and hematite, apparently cannot discriminate between magnetite and greigite having similar grain sizes. Paleomagnetists would thus benefit from other methods for the unambiguous identification of greigite.

In this article we report the results of a magnetic and geochemical study of some Cretaceous rocks from the North Slope basin of Alaska. The emphasis is on the identification and distribution of greigite, as well as on its contributions to the magnetization of the rocks and possibly to aeromagnetic anomalies. We also examine the relations among magnetic properties and the amounts of different sulfur species in the same specimens. Better understanding of the magnetic properties of greigite-bearing sediments may improve our ability to determine the distribution of different forms of sulfur for diagenetic and geochemical studies. A final goal is to determine the origin of the greigite using geochemical and sulfur isotopic methods.

MAGNETIC STRUCTURE AND OCCURRENCES OF GREIGITE

Greigite is the ferrimagnetic thiospinel of iron (Skinner, Erd, and Grimaldi, 1964; Ward, 1970; Vaughan and Craig, 1978). Sherman (1990) interpreted Mössbauer spectra of greigite to indicate (1) the presence of intermediate-spin Fe^{3+}, in addition to Fe^{2+}, to explain its magnetic moment of 2.2 ± 0.3 Bohr magnetons (μ_B; at 4.2°K), about half

that of magnetite (4.2 μ_B), and (2) a normal-spinel structure rather than an inverse-spinel structure as in magnetite (Spender, Coey, and Morrish, 1972).

Greigite has been reported as an authigenic mineral from many depositional settings, including lacustrine and swamp (Skinner, Erd, and Grimaldi, 1964; Giovanoli, 1979; Snowball, 1991; Snowball and Thompson, 1990a, b; Hilton 1990; Dell, 1972; Krs and others, 1990; Jedwab, 1967; Pye, 1981); marine (Morse and Cornwell, 1987; Horng and others, 1989; Freeman, Heller, and Rogenmoser, 1983; Berner, 1974; Bonev and others, 1989; Kalcheva and others, 1990; Snowball and Thompson, 1990b; Roberts and Turner, 1993); as well as estuarine and salt marsh environments (Suthill, Turner, and Vaughan, 1982; Cutter and Velinsky, 1988; Demitrack, 1985). Recently, intracellular particles of greigite ($\approx$75-nm diam) have been found in magnetotactic bacteria from brackish, sulfide-rich water and sediment (Mann and others, 1990).

The few paleomagnetic studies of greigite-bearing sediments report both stable and unstable remanent magnetizations. Stable remanence is recorded by greigite in Pliocene marls (Freeman, Heller, and Rogenmoser, 1983; Horng and others, 1989) and in marine and nonmarine sediments of Loch Lomond (Snowball and Thompson, 1990b). Viscous remanent magnetization in hemipelagic sediments was ascribed to greigite having superparamagnetic grain sizes (Brandsma, Lund, and Henyey, 1989; Leslie, Lund, and Hammond, 1990). Greigite is the cause of magnetic instability of Black Sea sediments (Kalcheva and others, 1990) and of Miocene nonmarine claystone (Krs and others, 1990). Giovanoli (1979) found that chemical remanent overprints attributed to greigite obscured a detrital magnetic record. In contrast, Suthill, Turner, and Vaughan (1982) concluded that magnetic contributions from greigite in some tidal-flat sediments were overwhelmed by stable remanence carried by detrital magnetite and titanomagnetite.

GEOLOGIC SETTING

The study area is in the eastern part of the Simpson Peninsula of the Arctic Coastal Plain, in the northern part of the North Slope basin (figs. 1, 2). Two major stratigraphic sequences occur in the basin: (1) Mississippian to Lower Cretaceous carbonate and clastic (Ellesmerian) rocks derived from sources to the north; and (2) overlying Lower Cretaceous to Quaternary clastic wedge (Brookian beds) derived from the ancestral Brooks Range to the south (fig. 3). These sequences are separated by an unconformity that represents rifting that opened an ocean basin to the north and that uplifted the basement to form the Barrow Arch (fig. 3). The regional geology of the north slope is summarized by Molenaar (1983), Bird (1987, 1988, 1991), and in papers in Tailleur and Weimer (1987) and Gryc (1988). Basin-scale groundwater flow from heat flow and subsurface temperatures is addressed by Deming and others (1992).

An important geologic feature in the study area is Simpson Canyon (figs. 2, 4), an ancient submarine canyon filled with marine mudstone of the Late Cretaceous Seabee Formation of the Colville Group. During an

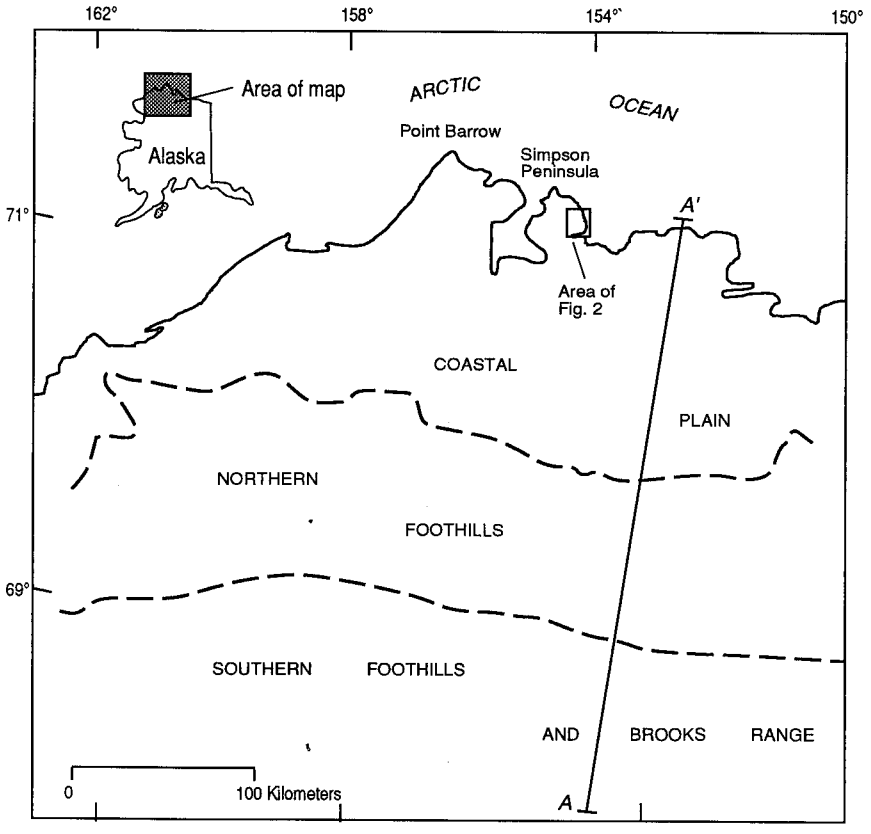

Fig. 1. Map of northern Alaska showing the location of Simpson Peninsula.

hiatus in Seabee deposition, the canyon was cut into the Seabee and the underlying Late Cretaceous Ninuluk Formation of the Nanushuk Group. In the study area, the pre-canyon Seabee is intercalated with nonmarine and marine sandstone, siltstone, and mudstone beds of the Ninuluk, and the boundary between the units is not easily defined (fig. 4). For this reason, the beds cut by the Simpson Canyon have been designated as undifferentiated Ninuluk and Seabee Formations by Robinson (1964). The Early Cretaceous marine Grandstand Formation conformably underlies the Ninuluk and Seabee sequence. Clay, silt, sand, and gravel of the Pliocene and Pleistocene Gubik Formation, as much as 30 m thick, cap the Cretaceous beds.

The study area encompasses the Simpson oil field. Oil is trapped mainly in sandstone outside the Simpson Canyon at depths of only about 100 m, perhaps in part by permeability contrasts across the canyon-wall unconformity. Seeps currently bring oil to the surface along fissures in

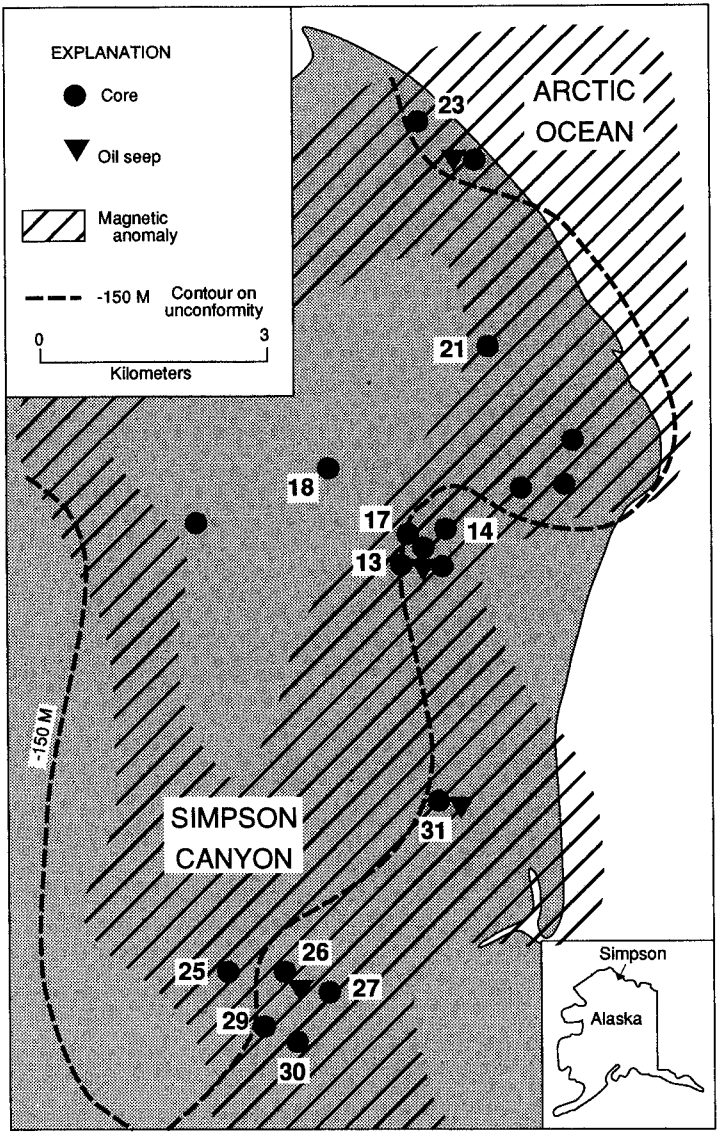

Fig. 2. Map of the Simpson Peninsula showing locations of cores, oil seeps, Simpson Canyon—a filled and covered submarine canyon—and the area of magnetic anomalies.

the permafrost and outline the eastern margin of the buried submarine canyon (fig. 2; Robinson, 1964). The oil is biodegraded and contains low amounts of sulfur (0.08-0.44 percent; Magoon and Claypool, 1981, 1988).

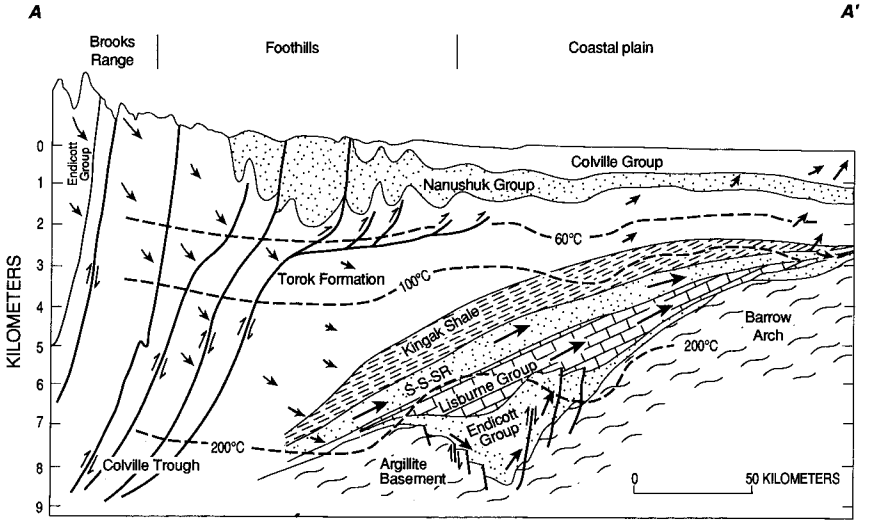

Fig. 3. Cross section of the North Slope basin showing major stratigraphic units and structure as well as inferred modern isotherms and ground-water flow paths (heavy arrows). The boundary between the Torok Formation and Kingak Shale is an unconformity that separates the Ellesmerian sequence from the overlying Brookian sequence (from Deming and others, 1992).

An aeromagnetic survey over the Simpson field (Donovan and others, 1988) detected magnetic anomalies having wavelengths of about 100 to 1000 m and amplitudes of about 1 to 50 nanoTesla (nT) apparently caused by magnetization in shallow sedimentary rocks (fig. 2). Steel casing in wellbores cannot account for the magnetic anomalies (see Boardman, 1987; Frischknecht, 1985), because development in the area is sparse, and drill sites are easily recognized. Donovan and others (1988) attributed the anomalies to hydrocarbon-induced formation of magnetic minerals.

METHODS

Sampling

The samples were taken from cores drilled between 1949 to 1951 for hydrocarbon assessment of the National Petroleum Reserve of Alaska (Robinson, 1964) and stored at room temperature since then. Sample numbers are denoted by core and depth in feet from the surface, as originally designated during drilling.

An initial goal was to identify the mineralogical source of the aeromagnetic anomalies. For this goal we collected samples over a range of 0.3 to 3 m of core having uniform lithology and color. Subsequent sampling, guided partly by scanning 900 m of core from 17 drill holes with a

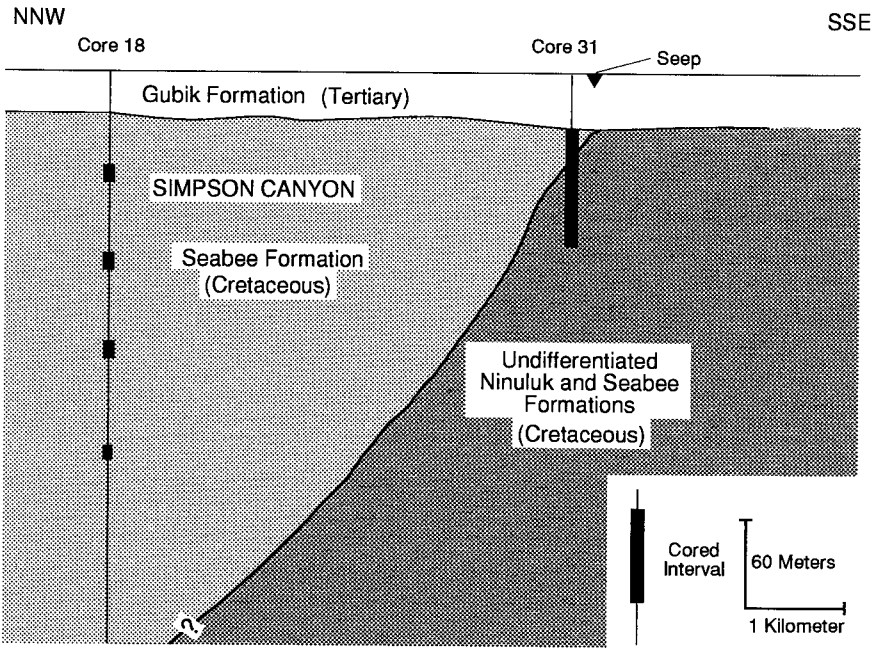

Fig. 4. Cross section showing cored intervals in cores 18 and 31.

hand-held magnetic susceptibility meter, expanded lithologic and geographic coverage, and it enabled detailed examination of some chemically heterogeneous or greigite-bearing intervals.

One hundred forty-five samples were collected from 12 cores (fig. 2), and from these more than 100 specimens were shaped into cubes for bulk magnetic-property measurements using a mason wheel and carborundum disks (table 1). Excess material from 45 of the trimmed specimens were used for magnetic-mineral separations so that magnetic mineralogy could be related to bulk magnetic properties of this subset of samples. After measurement of magnetic properties, 22 of these specimens were analyzed chemically to evaluate relations among magnetic properties, magnetic mineralogy, and geochemistry. In addition, magnetic minerals were identified from 70 other samples, 18 of which were also analyzed chemically.

We concentrated the studies on cores 31 and 18. Core 31 is within an area of the magnetic anomaly, lies close to an oil seep, and transects the canyon wall that separates the Seabee from beds of the undifferentiated Ninuluk and Seabee Formations. In contrast, core 18 is from the center of Simpson Canyon, remote from both seepage and the area of magnetic anomalies, and penetrated only the Seabee (figs. 2, 4).

TABLE 1

Summary of samples from cores, Simpson Penisula, Alaska

CORE	DEPTHS SAMPLED		FORMATION	SAMPLES	SPECIMENS ANALYZED			MAG MINERAL IDENTIFICATION					
	FEET	METERS		COLL.	CHEMISTRY	MAG PROPS	MAG MINS	G	G+FT	FT	SID	SID+G	SID+FT
31	115-186	35.1-56.7	S	12	13	7	12	12					
	190-353	57.9-107.6	NS	39	52	19	36	16	12	4	1	2	1
18	200-208	61.0-63.4	S	8	8	8	8	8					
	408-409	124.4-124.7	S	3	3	3	3	3					
	624-625	190.2-190.5	S	3	3	3	3		3				
	822-823	250.5-250.9	S	3	3	2	2		2				
13	80	24.4	Gu (ign)	1			1			1			
	132-355	40.2-108.2	S	4	3	3	4	3			1		
	393	119.8	S (ign)	1		1	1			1			
14	200-220	61.0-67.1	S	1	1		1		1				
	287-497	87.5-151.5	NS	9	4		4		1	3			
	565-1218	172.2-371.2	Gr	13	7	2	4	1		3			
17	201/405	61.3/123.4	S	2	2		1				1		
21	125-194	38.1-59.1	S	4	4	1	4	4					
23	212/506	64.4/154.2	S	2	2	2	2				2		
25	575	175.3	S	1	1						1		
26	129-317	39.3-96.6	NS	5	5	3	4	1		1	2		1
	575	175.3	Gr	1	1		1				1		
27	124-285	37.8-86.9	NS	13	13		7	1			5	1	
29	71/83	21.6/25.3	Gu	2	1		2		2				
	96-395	29.3-120.4	S	9	9	4	7	6	1				
30	118	36.0	S	1	1		1	1					
	242-408	73.8-124.4	NS	8	11	3	7	4			3		

Formation, in this and following tables: S, Seabee Formation that fills Simpson Canyon; NS, undifferentiated Ninuluk-Seabee; Gr, Grandstand; Gu, Gubik; ign, igneous rock fragment. Samp Coll, Number of samples collected; many samples were split into several specimens and analyzed using different chemical methods. Mag Props, Magnetic properties (Table 2). Mag Mins, Magnetic minerals, in this and following tables: G, Greigite; FT, Iron-titanium oxides; SID, Siderite.

Laboratory Procedures

Mineral identification.—Identification of the magnetic sulfide and oxide minerals required their concentration from bulk samples. This was done by immersing a permanent magnet in a slurry of sediment, water, and surfactant following dry disaggregation and dispersal of grains in an ultrasonic bath. Such separates, which concentrated magnetic particles ranging in size from less than 0.5 μm to more than 200 μm, were suitable for study by (1) X-ray diffraction (XRD) packed-powder techniques using Fe-Kα radiation, (2) the measurement of magnetization as a function of temperature to generate thermomagnetic curves, and (3) reflected-light microscopy. We further purified the magnetic separates using techniques similar to those described by Petersen, Von Dobonek, and Vali (1986). These separates were analyzed using scanning electron microscopy (SEM) with an energy-dispersive analyzer (EDA), X-ray powder-camera methods (using Fe-Kα radiation) of a few grains mounted on a gelatin fiber, and Mössbauer spectroscopy. Heavy liquids were also used to concentrate the magnetic and nonmagnetic heavy minerals from bulk samples. The identifications of magnetic minerals listed in the tables were based mainly on 95 thermomagnetic curves and examination of more than 100 polished grain mounts of magnetic separates.

Rock magnetic techniques.—Magnitudes of Natural Remanent Magnetization (NRM) and remanences induced in the laboratory were measured using a spinner magnetometer having a sensitivity of about 10^{-4} amperes/meter (A/m). Isothermal remanent magnetization (IRM) was imparted using an electromagnet capable of inductions to 0.93 T. Anhysteretic remanent magnetization (ARM) was generated in an alternating-field (AF) coil at a peak induction of 100 mT placed vertically in the ambient magnetic field of about 50,000 nT. AF demagnetization of remanence, in 7 to 12 steps to peak fields of 60 to 90 mT, was performed in a tumbling degausser. In the laboratory, magnetic susceptibility was measured using a device having a sensitivity of about 1.3×10^{-6} volume SI at 800 Hz in a field of 0.1 mT.

Geochemical techniques.—The forms and amounts of sulfur were determined by a sequential separation method described by Tuttle, Goldhaber, and Williamson (1986). Because the hot 6N HCl and stannous chloride treatment can potentially dissolve disulfide sulfur (the sulfur in pyrite), thereby elevating the recovered acid-volatile sulfur (AVS, the main sulfur type in greigite; Chanton and Martens, 1985; Cornwell and Morse, 1987), we used an extended sulfur speciation scheme combined with sulfur isotopy to test for such AVS artifact. The results (Rice, Tuttle, and Reynolds, 1993) indicate that very small amounts of disulfide sulfur (less than 5 percent of the disulfide sulfur) were recovered as AVS in the samples of canyon-fill Seabee. No such alterations were observed in the samples from the undifferentiated Ninuluk and Seabee sequence, probably because the contained sulfide minerals have different morphology and larger grain sizes than those in the canyon-fill sediment, as discussed below.

Concentrations of total carbon, organic carbon, carbonate carbon (by difference), and HCl-soluble iron were also measured. The amounts of total carbon and organic carbon were determined using an induction furnace coupled to a thermal-conductivity cell. Organic carbon was measured after the carbonate carbon was removed using dilute HCl; carbonate carbon was obtained by the difference between the total and organic carbon. The mean deviation of replicate analyses of total and organic carbon was $< \pm 3$ percent.

HCl acid-soluble iron (Fe_{HCl}) was measured from the 6N HCl and stannous chloride solution in the first step of the sulfur-separation scheme using standard flame atomic absorption methods with a reproducibility of ± 10 percent. Such acid-soluble iron represents that in monosulfide, carbonate, and clay. The amounts of iron in disulfide minerals (Fe_{di}) and in monosulfide (Fe_{av}, approximating the Fe in greigite) were calculated from disulfide S and AVS, respectively, assuming respective stoichiometric FeS_2 and Fe_3S_4. These values, with Fe_{HCl}, were used to calculate the reactive Fe (Fe_r) and the degree of sulfidization (DOS_r):

$$Fe_r = Fe_{HCl} + Fe_{di} \quad (1)$$

$$DOS_r = [Fe_{di} + Fe_{av}]/Fe_r \quad (2)$$

The parameter Fe_r is intended as a measure of iron that was available for sulfidization by H_2S. The Fe_r term operationally defined above differs from the reactive Fe defined by Berner (1970) as Fe leached by 12 N HCl boiled for one minute. DOS_r is the fraction of reactive iron that has been sulfidized. As demonstrated by Canfield, Raiswell, and Bottrell (1992), such terms for reactive and sulfidized iron may not closely reflect iron-sulfur reactions during early diagenesis, because the Fe leached in the laboratory may not have been readily available for sulfidization in the sediment.

The isotopic compositions of the sulfur products from the separation scheme (Ag_2S or $BaSO_4$) were determined by conversion of the products to SO_2, which was then analyzed using mass spectrometry techniques. Similarly, isotopic compositions were obtained from a commercial laboratory following the separations of sulfur species by us (AVS, disulfide S, sulfate S, and organosulfur) or by the laboratory (AVS, sulfate S, and disulfide S). All sulfur isotopic results are reported relative to the Cañon Diablo Troilite (CDT) standard. Carbon and oxygen isotopic results (relative to the PDB standard) were determined on CO_2 converted from carbonate minerals.

IDENTIFICATION, DISTRIBUTION, AND OCCURRENCES OF IRON SULFIDE, IRON OXIDE, AND IRON CARBONATE MINERALS

Iron Sulfide Minerals

Identification.—Greigite and pyrite were identified using XRD and Mössbauer methods (figs. 5, 6). The Mössbauer spectrum of a sample of

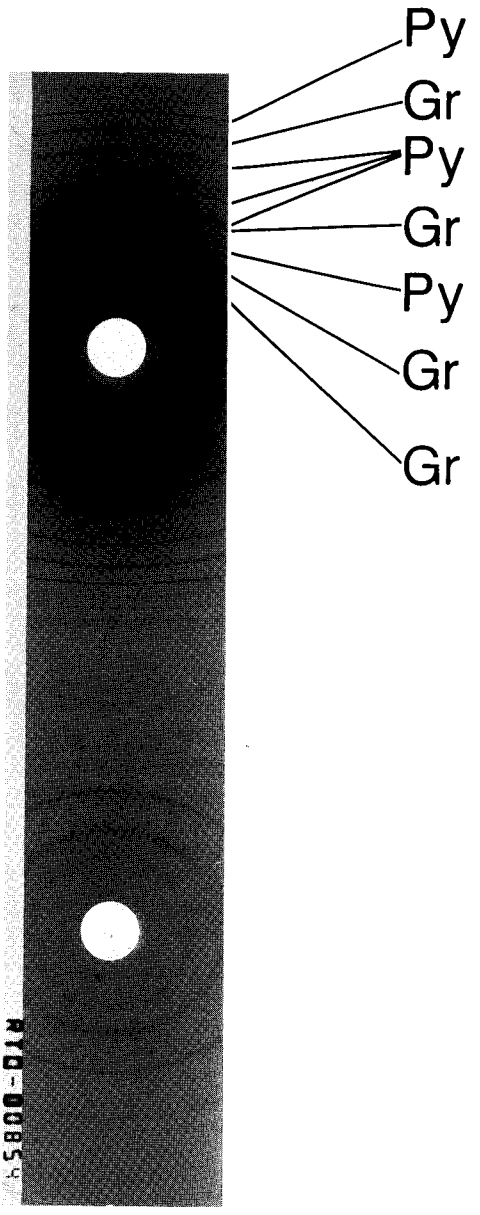

Fig. 5. X-ray diffraction pattern of magnetic separate from sample 31-256 which was mounted on a gelatin fiber and exposed for 8 hrs. Pyrite (Py) is intimately mixed with and could not be physically separated from greigite (Gr).

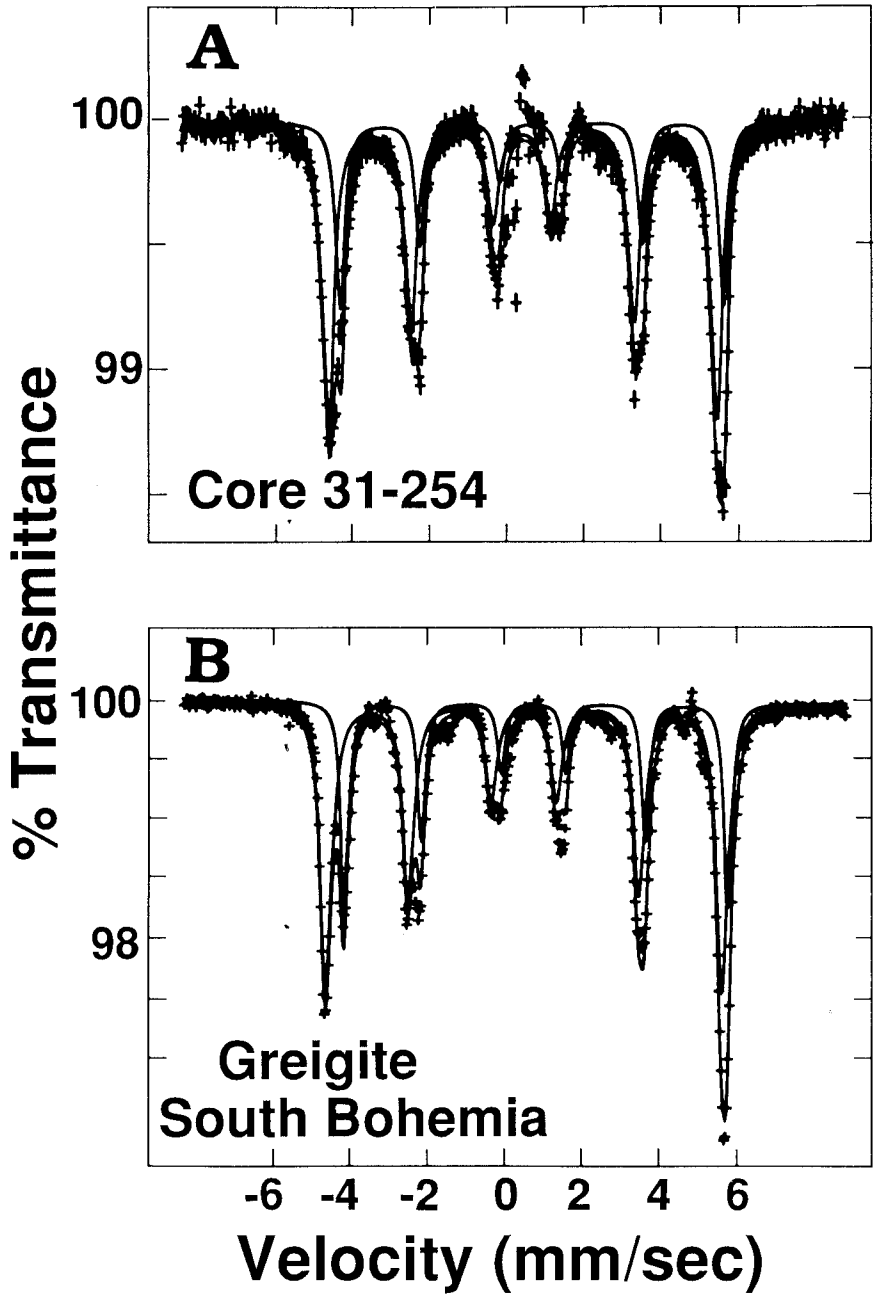

Fig. 6. Mössbauer spectra of magnetic separates that contain greigite: (A) sample from the undifferentiated Ninuluk and Seabee Formations which also contains pyrite; (B) sample from Bohemia which also contains about 2 percent ferrimagnetic pyrrhotite.

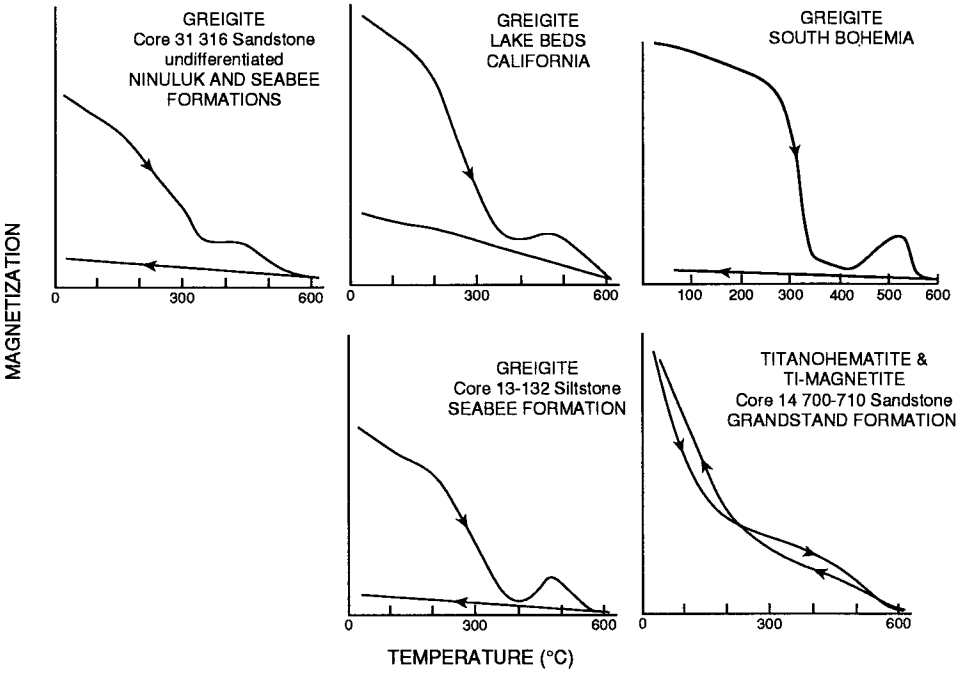

Fig. 7. Thermomagnetic curves of magnetic separates heated in air using a 0.93 T field.

nearly pure greigite (Krs and others, 1990; Hoffmann, 1992) from the Sokolov basin, Bohemia, is shown for comparison.

Magnetic separates that contain predominant greigite, as confirmed by XRD, have characteristic thermomagnetic curves (fig. 7). When heated in air, samples abruptly lose most of their magnetization between 200° and about 350°C. The thermomagnetic curves are reversible to 250°C but irreversible at higher temperatures. The increase in magnetization above about 350°C is caused by the oxidation of iron sulfide to magnetic iron oxide. In the Bohemian sample, which initially lacks disulfide, maghemite and hematite are produced via the oxidation of pyrite, marcasite, and hexagonal pyrrhotite that formed from greigite above about 300°C (Krs and others, 1992). Under heating in air, the further oxidation of the sulfide and maghemite to hematite results in cooling paths far below the heating paths. Such curves resemble a curve for a greigite separate from Loch Lomond generated in air by Snowball and Thompson (1990b). In our experience, thermomagnetic analysis in a nitrogen-gas environment (see Snowball and Thompson, 1990b) does not elucidate the thermomagnetic properties of greigite; we generated curves having vastly different shapes using different flow rates of nitrogen. At high-flow rates and

temperatures above 300°C, magnetic iron oxide either continues to form, or that formed at lower temperatures persists, and the resulting curve shows little evidence for the original greigite. We thus recommend an air environment for the thermomagnetic analysis of greigite, because the products of the oxidation and breakdown of greigite in air generate a diagnostic thermomagnetic curve (see Schwarz, 1974, for comparisons with pyrrhotite).

Greigite was detected petrographically on the basis of characteristic colors and reflections from magnetic separates in polished grain mounts, although individual particles in most samples were commonly much too small (<1 μm) to identify from optical properties alone. The identification of greigite was confirmed in most such samples using thermomagnetic analysis. Larger particles of greigite, as much as 5 μm in diameter, occur in marine mudstone that fills the Simpson Canyon.

Pyrrhotite occurs sparsely in magnetic separates in samples from both the canyon-fill Seabee Formation and the undifferentiated Ninuluk and Seabee Formations. The predominance of greigite in these magnetic separates precluded XRD and thermomagnetic confirmation of ferrimagnetic pyrrhotite. In two magnetic separates (from core 31, samples 241-252 and 309), antiferromagnetic pyrrhotite was indicated in thermomagnetic curves by an increase in magnetization at about 200°C during heating (see Schwarz, 1974).

Distributions and occurrences.—Authigenic greigite is widespread in the study area. It was found in every core, except cores 17, 23, and 25, examined for siderite concretions only (table 1). Greigite is ubiquitous in marine mudstone of the Seabee and common in each lithology of the undifferentiated Ninuluk and Seabee (tables 1, 2). Greigite is also present with detrital magnetic oxides in the Gubik and rarely in the Grandstand Formations.

The occurrences, textures, and sizes of the iron sulfide minerals in the canyon-fill Seabee Formation differ in some important ways from those characteristics in the undifferentiated Ninuluk and Seabee Formations. In the canyon-fill Seabee, greigite occurs mixed with fine-grained pyrite (typically <20 μm) and commonly within the cell lumens and on coalified surfaces of some fossil plant fragments which thus could be concentrated magnetically. Framboidal pyrite is also common in heavy-mineral separates.

In undifferentiated Ninuluk and Seabee rocks, aggregates of fine-grained greigite are commonly associated with pyrite, but some samples that contain pyrite are devoid of greigite. Occurrences of greigite in plant fragments are rare even though such fragments are common. Framboidal and fine-grained euhedral pyrites are surrounded or cemented by large crystals or composite grains of pyrite, of marcasite, or of pyrite-marcasite in samples from core 31 covering depths of 64 to 77 m ($\approx$211-252 ft) and 86 to 91 ($\approx$283-297 ft) (fig. 8). In a few samples, greigite aggregates surround and appear partly to replace the margins of large pyrite and rare pyrite-marcasite grains. Large pyrite grains that

cement fine-grained euhedral and framboidal pyrite also occur in two samples from the overlying Seabee (31 115-125 and 31 166-175).

Iron Oxide Minerals

Detrital grains of the magnetite-ulvospinel and hematite-ilmenite solid-solution series are present but sparse in each formation (table 1). The dominant Fe-Ti oxide minerals in the magnetic separates are angular to subrounded, optically homogeneous, ferrimagnetic titanohematite grains, typically 5 to 50 μm in diameter. These grains have Curie temperatures between 150° to 220°C, indicating compositions between about 59 and 51 mol percent ilmenite, respectively (Nagata and Akimoto, 1956). Such textural and chemical characteristics suggest the derivation of these Fe-Ti oxide grains from intermediate-composition igneous rocks (see Reynolds, 1977; Butler and Lindsay, 1985).

Petrographic observations suggest that detrital magnetite has largely been destroyed by the postdepositional dissolution of iron. The earlier presence of magnetite is strongly implied by (1) relicts of former titanomagnetite as fragile grains that consist of TiO_2 lamellae along {111} crystallographic planes (fig. 8) and (2) abundant unaltered magnetite within protective ferromagnesian minerals in an igneous-rock fragment from the Seabee Formation. Evidence for the replacement of magnetite by pyrite is rare. The persistence of titanohematite under conditions that deplete magnetite has been documented in other sedimentary rocks (Reynolds, 1982; Larson, Patterson, and Evanoff, 1990; Canfield, Raiswell, and Bottrell, 1992).

Siderite

Concretions and lenses of siderite were collected selectively, because they have high magnetic susceptibility and because they contain fine-grained pyrite as a possible diagenetic record of iron-sulfide formation. The siderite occurs in most cores, but it is extremely sparse, comprising less than 0.1 percent of the cores.

ROCK MAGNETIC RESULTS

NRM and Magnetic Susceptibility

Greigite dominates the bulk magnetic properties of the Late Cretaceous units (table 2). Specimens that contain greigite only (G-group) have greater magnitude of NRM and generally greater MS than specimens that contain detrital magnetic oxides as the only observed magnetic minerals (FT-group) (fig. 9). Most specimens with mixtures of greigite and Fe-Ti oxide grains have intermediate values of MS and NRM. Specimens of siderite plot in a cluster of high MS and low NRM, and those having some greigite or magnetic Fe-Ti oxide plot between this cluster and the G-group and FT-group fields, respectively. Magnetic-property values lack apparent relations to lithic types.

TABLE 2

Summary of magnetic data, Cretaceous units, Simpson Peninsula, Alaska

Core & Sample	Chem Table 3	Magnetic Mineral	Lith	Formation-Dep Envir	MS SI Vol x 10^{-4}	NRM A/m x 10^{-3}	MDI-NRM (mT)	Q	ARM A/m x 10^{-3}	ARM/MS	SIRM (A/m)	SIRM/MS (A/m)	B_{cr} (mT)	SIRM/ARM
14 700-710A	*	FT	SS	Gr MAR	0.77	4.34	13	1.2	6.10	79	0.21	2771	39	35
14 700-710B	*	FT	SS	Gr MAR	0.43	1.69	UNST	0.9	8.04	189	0.24	5682	44	30
26 129-130A	*	FT	Sltst	NS MAR	1.00	6.23	20	1.4	6.27	63	0.37	3730	48	59
26 186A		FT+SID	SS	NS MNM	6.03	2.86	20	0.1	8.59	14	0.41	673	42	47
31 211-219	*	FT	SS	NS MNM	3.32	2.77		0.2			0.89	2675	43	
31 228B	*	FT+SID	SS	NS MNM	5.32	1.07	31	0.04	7.15	13	0.27	505	45	38
31 263-274A		FT+G	Sltst	NS MAR	0.57	1.99	UNST	0.8	6.38	111	0.34	6003	53	54
31 276B		FT	Sltst	NS MAR	0.42	0.29		0.2	1.72	41				
31 276A	*	FT+G	Sltst	NS MAR	1.54	0.86	UNST	0.1	8.65	56	0.44	2857	52	51
31 334		FT+G	Sltst	NS NM	1.30	1.06	UNST	0.2	11.75	90	0.61	4660	59	52
31 339		FT+G	Sltst	NS NM	1.51	3.48	49	0.5	17.80	118	1.57	10425	60	88
31 343 (Ash)		FT	Ash	NS NM	1.14	1.72	UNST	0.3	4.08	36	0.64	5565	75	156
13 132	*	G	Sltst	S MAR	9.10	101.00		2.5						
18 200-201E	*	G	Mudst	S MAR	4.46	55.85	36	2.8	80.25	180	29.46		45	367
18 200-201F		G	Mudst	S MAR	3.89	35.79		2.0						
18 204-205D	*	G	Mudst	S MAR	7.63	93.26	40	2.7	103.40	135	64.56	84580	48	624
18 204-205E		G	Mudst	S MAR	10.40	153.00		3.2						
18 207-208A	*	G	Mudst	S MAR	6.41	73.14		2.5						
18 207-208B		G	Mudst	S MAR	8.64	112.30	41	2.9	117.80	136	84.75	98056	52	719
18 408-409B	*	G	Mudst	S MAR	3.07	50.41	19	3.6	22.56	73	15.33	49935	50	680
18 308-409C		G	Mudst	S MAR	2.14	2.34		0.2						
18 624-625A	*	G+FT	Mudst	S MAR	2.26	5.13	46	0.5	14.49	64	4.70	20855	52	325
18 624-625B		G+FT	Mudst	S MAR	2.67	5.25		0.4						
18 822-823C	*	G+FT	Mudst	S MAR	2.77	13.19	38	1.1	22.14	80	7.30	26337	42	330
18 822-823D	*	G+FT	Mudst	S MAR	3.11	14.71		1.0						

21 194B		G	Mudst	S MAR	16.89	175.70	49	2.3	523.90	310	217.20	128597	61	415
29 335C		G	Mudst	S MAR	5.74	74.69	40	2.9	188.00	327	42.07	73254	58	224
29 366A	*	G	Mudst	S MAR	11.43	186.00	44	3.6	246.00	215	199.20	174278	63	810
29 366E1	*	G	Sltst	S MAR	2.82	21.70	38	1.7	62.70	222	9.42	33392	55	150
29 395		G	Sltst	S MAR	2.73	21.12	UNST	1.7	60.25	221	10.16	37257	57	169
30 264.5		G	SS	NS MNM	3.84	10.00	40	0.6	38.80	101	4.29	11166	58	111
30 265-266	*	G	SS	NS MNM	5.42	73.90	43	3.0	117.00	216	29.75	54899	56	254
30 267B	*	G	SS	NS MNM	3.39	52.30	47	3.4	80.30	237	25.20	74249	62	314
31-130		G	Mudst	S MAR	6.72	127.00		4.2						
31 254B	*	G	SS	NS MAR	5.66	65.20		2.5			50.70	89544	62.5	
31 254C		G	SS	NS MAR	8.32	98.15	50	2.6	267.60	322	79.01	94987	61	295
31 255-256B	*	G	SS	NS MAR	2.12	19.35	45	2.0	48.29	228	13.89	65550	58	287
31 263-274B	*	G+FT	Sltst	NS MAR	2.35	11.85	50	1.1	25.30	108	8.25	35074	61	326
31 321B		G+FT	SS	NS MNM	1.15	3.91		0.8			1.48	12881	71	
31 321C		G+FT	SS	NS MNM	1.72	3.07	UNST	0.4	15.31	89	1.93	11183	73	126
31 331	*	G	SS	NS MNM	2.88	20.80	43	1.6	38.70	134	15.60	54204	58	403
13 238A		SID	Sltst	S MAR	23.00	1.51	37	0.01	4.59	2.0	0.94	407	58	204
23 212B		SID	Mudst	S MAR	22.66	0.69	33	0.01	3.23	1.4	0.94	416	63	292
23 506-1B		SID	Mudst	S MAR	25.63	0.70	UNST	0.01	3.14	1.2	0.46	178	55	145
26 317B		SID+G	SS	NS MNM	25.39	7.03	35	0.06	13.76	5.4	8.01	3156	61	582

Chem table 3, * denotes specimens analyzed chemically (table 3). Lith, lithology, in this and following tables: SS, sandstone, Sltst, siltstone; Mudst, mudstone. Dep Envir, depositional environment, in this and following tables: MAR, marine; MNM, indeterminant marine or nonmarine; NM, nonmarine. MS, magnetic susceptibility. NRM, natural remanent magnetization in A/m, Amperes/meter. MDI-NRM median destructive inductance of NRM in mT, milliTesla; UNST, unstable, MDI could not be determined. Q, Koenigsberger ratio, the magnitude of NRM/magnitude of induced magnetization, using an induction of 57,000 nT. ARM, anhysteretic RM. SIRM, saturation isothermal RM. B_{cr}, coercivity of remanence.

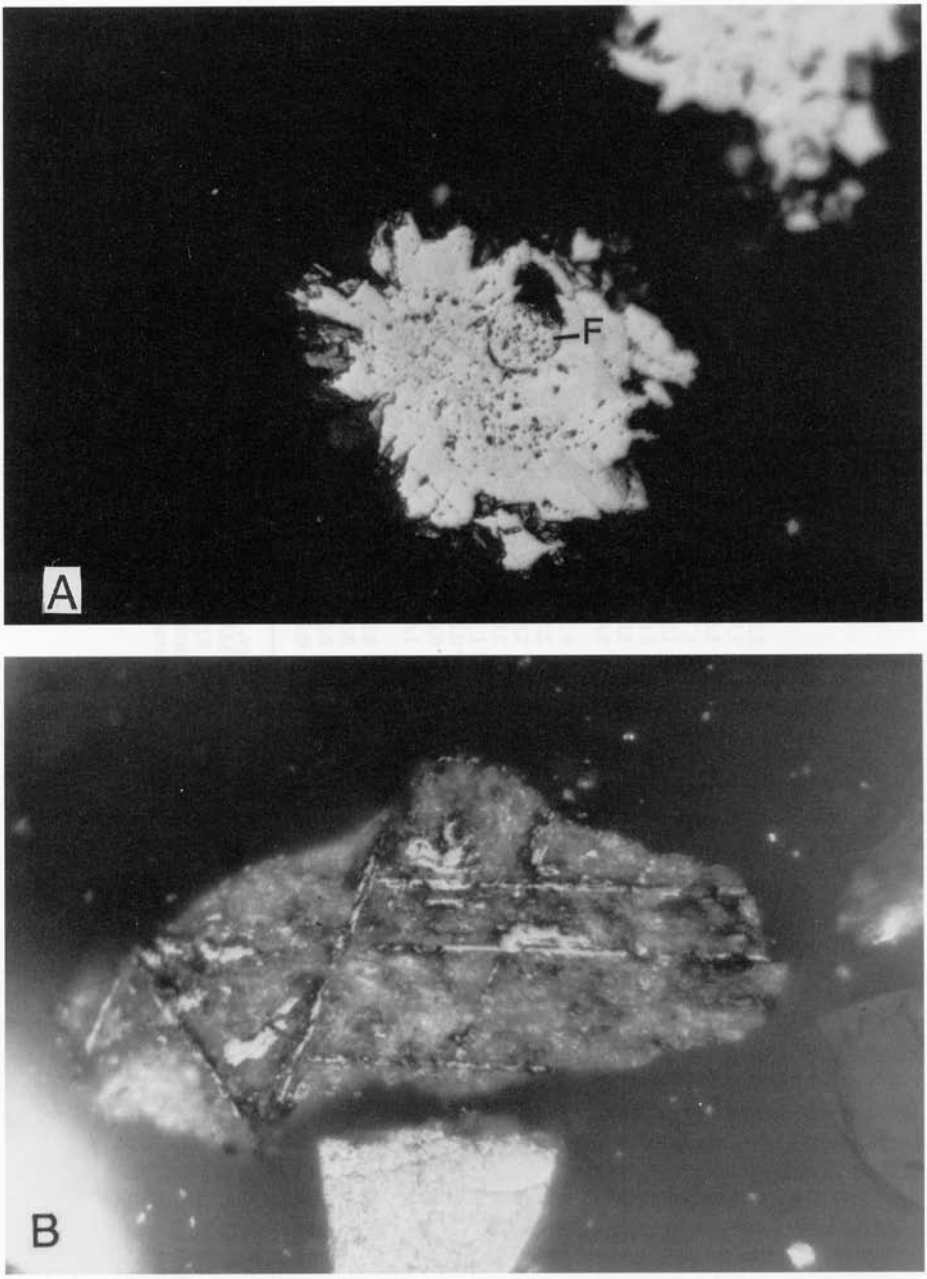

Fig. 8. Polished surface photomicrographs. (A) Pyrite and marcasite surround framboidal pyrite (round object indicated by "F"). From the undifferentiated Ninuluk and Seabee Formations, core 31, sample 211–215. (B) Former detrital titanomagnetite, in which the magnetite has been altered by removal of iron to leave titanium-rich residue between former ilmenite lamellae. From the undifferentiated Ninuluk and Seabee, core 31, sample 353. Field of view in both photomicrographs is 160 μm.

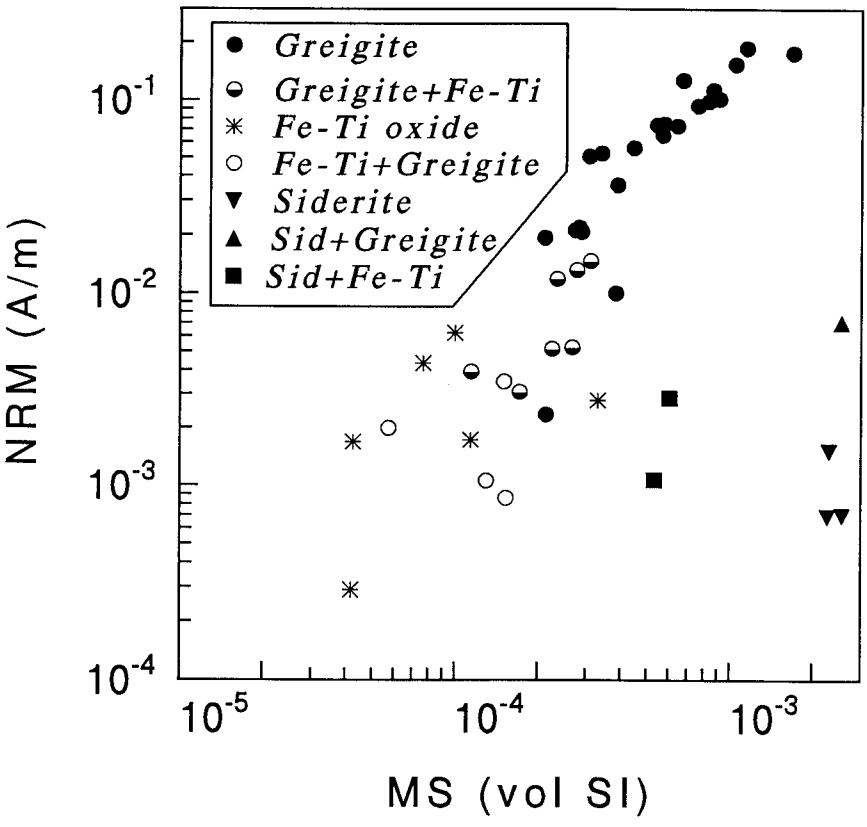

Fig. 9. Plot of magnitude of natural remanent magnetization (NRM) against magnetic susceptibility (MS), keyed to magnetic minerals. When listed together (for example, "Greigite+Fe-Ti") the first mineral is qualitatively judged the more abundant on the basis of petrographic examination of magnetic-mineral separates from sediment that enclosed the magnetic specimen.

Stability of NRM, Coercivity, and Discrimination Among Magnetic Carriers

Most G-group specimens were stable to AF demagnetization—their magnetization vectors showed nearly straight-line decay through peak inductions of 60 to 80 mT (fig. 10). In contrast, most FT-group specimens showed erratic response to lower AF inductions. Such unstable behavior usually precluded the determination of the median destructive inductance (MDI, the AF induction at which half the NRM is lost) which is a measure of magnetic coercivity. The three specimens of the FT group for which the MDI could be determined had values ($\leq$20 mT), much less than those of nearly all G-group specimens (MDI typically $>$35 mT) (table 2).

The acquisition and the backfield removal of IRM also indicate an overall higher coercivity in the G-group than in the FT-group specimens.

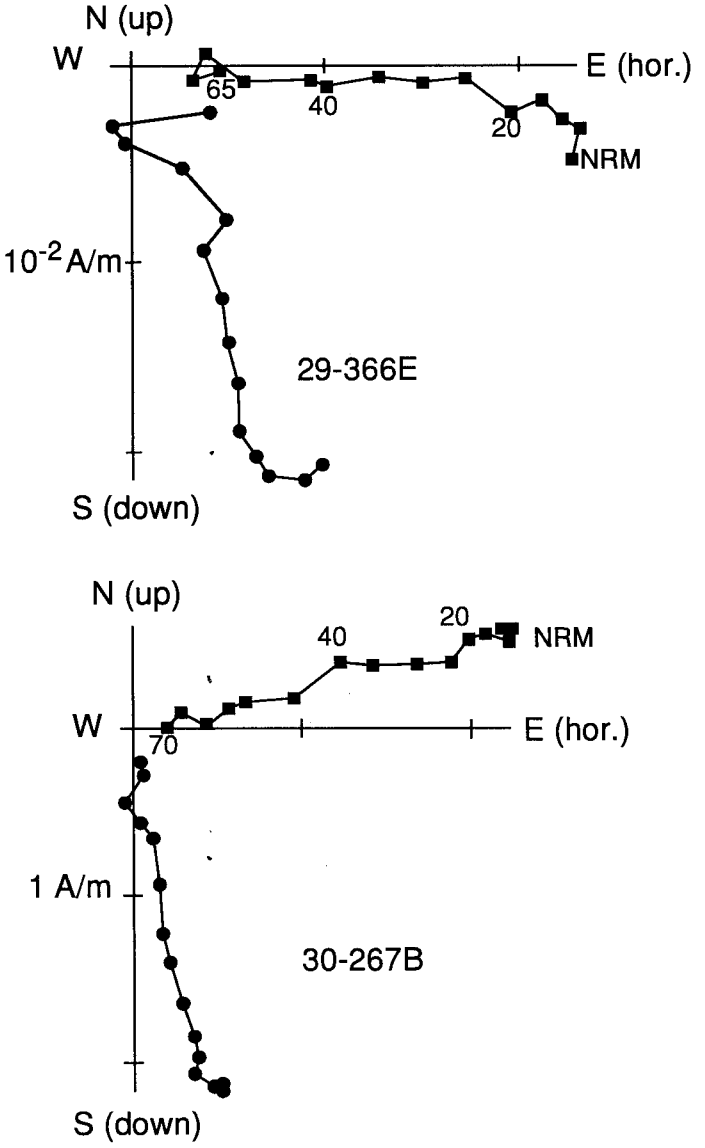

Fig. 10. Orthogonal demagnetization diagrams (see Zijderveld, 1967) of specimens that contain greigite as the only identified magnetic mineral. Circles (squares) represent projections of the magnetic vector on the horizontal (vertical) planes.

Although the shapes of the IRM acquisition curves are similar and show saturation by applied inductions of less than 0.3 T for both groups, G-group specimens acquire about 20 percent of the SIRM at 0.05 T, whereas FT-group specimens acquire between about 35 and 50 percent at this induction (fig. 11). This difference is also expressed in the backfield curves: G-group specimens have convex-upward curves, and most have values of coercivity of remanence (B_{cr}) greater than 0.05 T; whereas FT-group specimens have concave-upward curves, and most have B_{cr} values less than 0.05 T (fig. 11). The differences in B_{cr} values are subject to complicating factors, especially the content of high-coercivity hematite that increases the B_{cr} values in some FT-group specimens. We attribute the high B_{cr} value (0.075 T) in one FT-group specimen from a thin bed of volcanic ash (table 2, 31-343) to petrographically observed hematite that formed before deposition during cooling and high-temperature oxidation of the associated magnetite.

The G- and FT-group specimens are discriminated most clearly on the basis of the SIRM/MS ratio (table 2; fig. 12): G-group specimens range from about 11 kA/m to 175 kA/m, whereas FT-group specimens have values less than 6 kA/m. A similar result is reported by Snowball and Thompson (1990b) and by Roberts and Turner (1993). The presence of siderite, even when coexisting with greigite in a specimen, greatly depresses SIRM/MS (table 2). Plots of ARM against MS (fig. 13) for the non-siderite-bearing specimens define a rather tight trend—the greigite-bearing specimens having ARM values above those of the FT-group specimens. The plots, however, clearly do not reveal different slopes for the two groups and thus do not separate the G-group from FT-group specimens on the basis of their grain-size differences; such plots may reflect equivalent differences in grain sizes among magnetites (Banerjee, King, and Marvin, 1981).

GEOCHEMICAL RESULTS

Contents of Sulfur, Carbon, and Iron

Geochemical results for the analyzed forms of sulfur, carbon, and iron are considered in terms of (1) the lithologies and depositional environments (dominantly mudstone of the marine Seabee Formation vis-a-vis dominantly coarser marine and nonmarine sediments of the undifferentiated Ninuluk and Seabee Formations), and (2) the dominant magnetic mineral in a sample (table 3). Average values of elemental contents and their generally high standard deviations are shown for the comparative sets in table 4. The high dispersions are related mainly to the mixtures of lithology, formation, or magnetic mineralogy within the averaged sets (table 4).

Total sulfur content in the undifferentiated Ninuluk and Seabee Formations (0.44 wt percent) is not significantly different from that in the Seabee (0.31 wt percent), according to the nonparametric Mann-Whitney U test at the 0.05 probability level. Significantly different distributions of

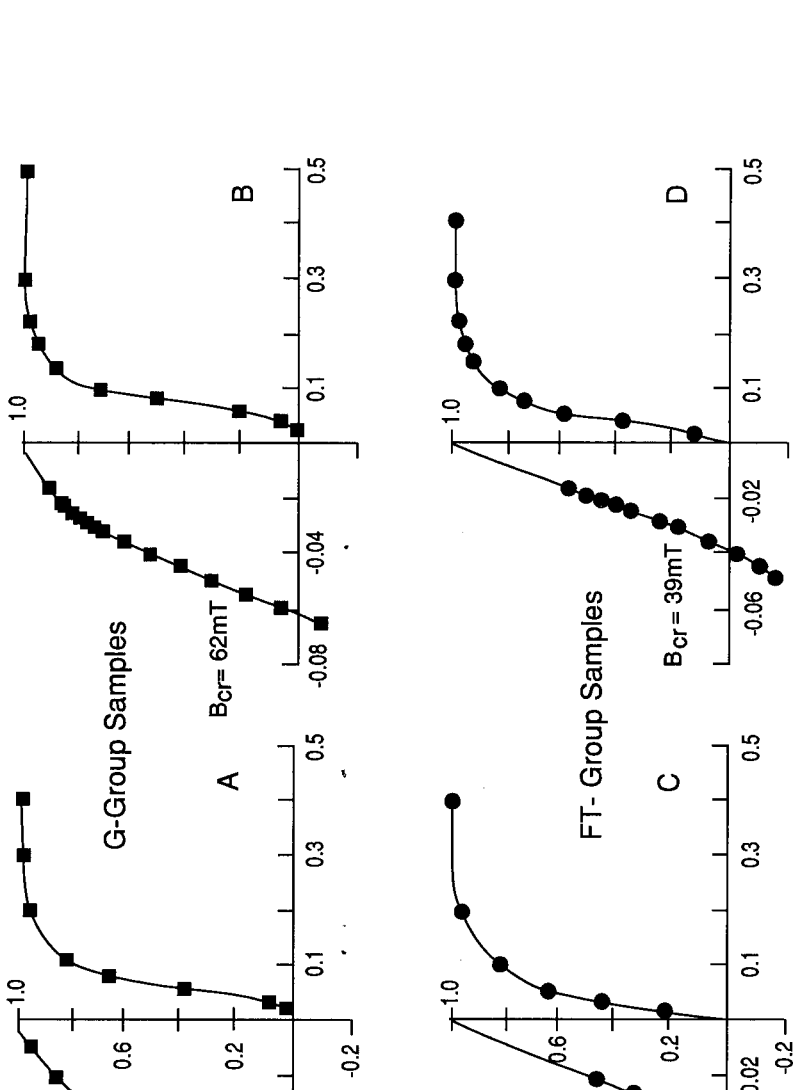

Fig. 11. Curves showing the acquisition of isothermal remanent magnetization (IRM) and the removal of the saturation IRM with the application of a backfield IRM (negative field values). Specimens that contain greigite only (G-group) denoted by squares; those that contain Fe-Ti oxides only (FT-group) by circles.

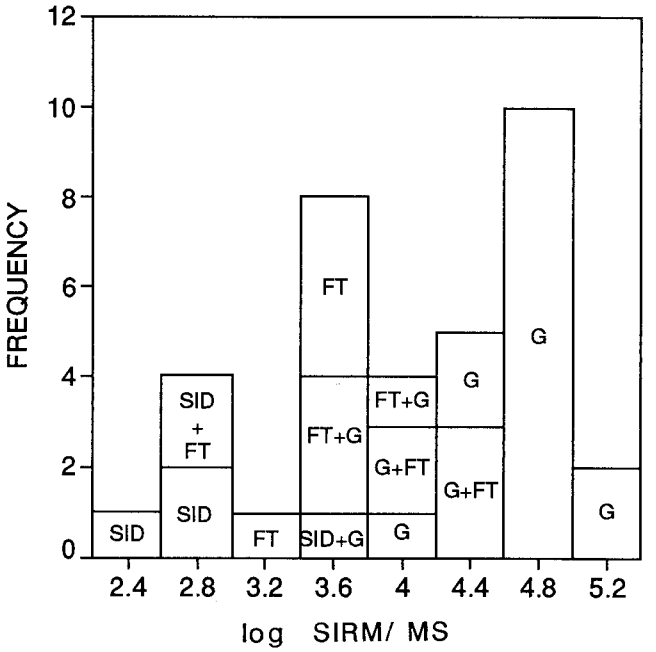

Fig. 12. Histogram of the ratio saturation isothermal remanent magnetization (SIRM) to magnetic susceptibility (MS). Abbreviations as in table 1. The higher values are found in greigite-bearing specimens.

AVS and disulfide sulfur in these units, however, indicate different residences for the sulfur. The Seabee contains higher AVS (0.08 wt percent or 26 percent of the total S) than the undifferentiated Ninuluk-Seabee (0.05 wt percent or 11 percent of total S) but less disulfide sulfur (0.14 wt percent or 45 percent of the total S; and 0.34 wt percent or 77 percent of the total S, respectively). G-group specimens contain 0.08 wt percent AVS, and FT-group specimens contain 0.02 wt percent AVS, implying that greigite might be present in some FT-group specimens but in amounts masked petrographically and magnetically by the detrital oxides. Contents of sulfate S, probably generated by the oxidation of greigite and pyrite, are low and vary without consistent relation to AVS or disulfide S contents.

The range of organic-carbon contents in the Seabee Formation is extremely narrow, and the average content (1.1 wt percent) is greater than in the undifferentiated Ninuluk and Seabee Formations (0.49 wt percent). Greigite-bearing samples have a higher average organic-carbon content than those devoid of greigite. Organic-carbon contents correspond closely to sediment grain size: Average values are highest in mudstones (1.0 wt percent), intermediate in siltstone (0.88 wt percent),

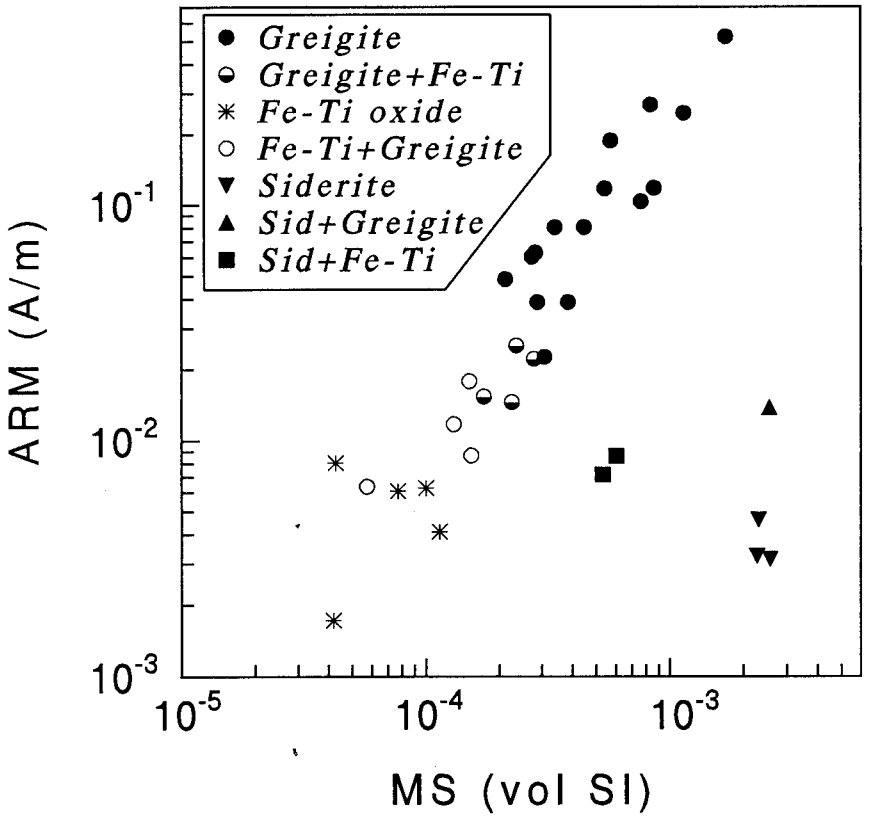

Fig. 13. Plot of magnitude of anhysteretic remanent magnetization (ARM) against magnetic susceptibility (MS), keyed to magnetic minerals. Abbreviations as in figure 8.

and lowest in sandstone (0.23 wt percent). Carbonate-carbon content in sandstone (0.89 wt percent) is much higher than in siltstone and mudstone (each about 0.32 wt percent).

Ratios of reduced sulfur (disulfide S plus AVS) to organic carbon (S/C ratios) may provide clues to depositional conditions and postdepositional alterations of the Cretaceous beds (Gautier, 1986; 1987; Dean and Arthur, 1989). One basis for such clues are observed S/C ratios in Quaternary and modern normal marine sediments (≈ 0.36; Raiswell and Berner, 1986; Lin and Morse, 1991) which reflect the control of organic carbon on the production of sulfide minerals during diagenesis, mainly by bacterial sulfate reduction (Sweeney and Kaplan, 1973; 1980). These samples, whether considered as one suite or as different subsets, do not follow the relation found in normal marine mud (fig. 14). For example,

TABLE 3

Summary of geochemical data, Cretaceous units, Simpson Peninsula, Alaska

Core & Sample	Mag Min	Lith	Formation Dep Envir	Fe_{HCl}	Fe cr sol	Organic C	Carb C	S tot-sum	S/C	AVS	Di S	SO_4 S	S org	S in OM
13 132*	G	Slts.	S MAR	2.8	0.12	0.59	0.56	0.22	0.34	0.12	0.08	0.01	0.01	0.8
18 200-201E*	G	Mdst.	S MAR	2.9	0.07	0.91	0.44	0.06	0.05	0.03	0.02	0.01	0.007	
18 200-201	G	Mdst.	S MAR	0.74	0.09	0.91	0.38	0.14	0.11	0.05	0.05	0.03	0.01	0.5
18 204-205D*	G	Mdst.	S MAR	3.1	0.11	0.98	0.27	0.18	0.14	0.08	0.06	0.03	0.01	0.5
18 204-205	G	Mdst.	S MAR	3.1	0.14	1.0	0.24	0.26	0.19	0.10	0.09	0.06	0.01	0.5
18 207-208A*	G	Mdst.	S MAR	3.0	0.13	1.0	0.17	0.20	0.14	0.07	0.07	0.05	0.01	0.5
18 408-409B*	G	Mdst.	S MAR	4.3	0.12	0.95	0.32	0.26	0.16	0.05	0.01	0.11	0.007	
18 408-409	G	Mdst.	S MAR	1.1	0.29	0.95	0.17	0.63	0.45	0.07	0.36	0.19	0.01	0.5
21 182A	G	Mdst.	S MAR	3.9	0.09	0.94	0.56	0.34	0.26	0.18	0.06	0.09	0.01	0.5
21 182B	G	Mdst.	S MAR	3.9	0.09	0.99	0.51	0.37	0.26	0.20	0.06	0.10	0.01	0.5
29 366A*	G	Slts.	S MAR	3.1	0.20	1.24	0.45	0.35	0.23	0.14	0.15	0.05	0.01	0.4
29 366E1*	G	Slts.	S MAR	2.6	0.09	2.3	0.64	0.06	0.02	0.02	0.02	0.01	0.01	0.2
30 265-266*	G	Ss.	NS MAR	2.9	0.23	0.25	0.16	0.36	1.4	0.09	0.25	0.01	0.01	2
31 115-125	G	Mdst.	S MAR	3.8	0.18	1.1	0.45	0.20	0.13	0.02	0.12	0.05	0.01	0.5
31 130*	G	Mdst.	S MAR	4.7	0.27	0.98	0.32	0.50	0.40	0.13	0.26	0.09	0.02	1
31 144-155	G	Mdst.	S MAR	4.0	0.35	0.93	0.29	0.21	0.19	0.08	0.11	0.02	0.01	0.5
31 160A	G	Mdst.	S MAR	3.9	0.24	1.0	0.18	0.46	0.33	0.10	0.24	0.11	0.01	0.5
31 160B	G	Mdst.	S MAR	3.9	0.80	1.1	0.31	0.17	0.10	0.06	0.05	0.05	0.01	0.5
31 166-175	G	Mdst.	S MAR	3.9	0.38	1.10	0.14	0.38	0.23	0.07	0.18	0.11	0.02	0.9
31 175-186	G	Mdst.	S MAR	3.8	0.12	1.0	0.98	0.17	0.06	0.02	0.04	0.10	0.01	0.5
31 254B*	G	Ss.	NS MAR	3.2	0.44	0.34	0.14	0.56	1.6	0.09	0.44	0.03	0.007	
31 255C	G	Ss.	NS MAR	2.8	0.08	0.27	0.17	0.07	0.22	0.02	0.04	0.007	0.01	0.5
31 255-256B*	G	Ss.	NS MAR	2.7	0.06	0.40	0.24	0.05	0.13	0.02	0.03	0	0.007	
31 283	G	Mdst.	NS MNM	2.9	0.54	1.2	0.12	0.49	0.37	0.07	0.36	0.04	0.02	0.9
31 331*	G	Ss.	NS MNM	3.5	0.05	0.03	0.64	0.04	1.0	0.02	0.01	0.01	0.007	
18 624-625	G+FT	Mdst.	S MAR	4.5	0.36	0.93	0.36	0.67	0.55	0.05	0.46	0.15	0.01	0.5
18 624-625A*	G+FT	Mdst.	S MAR	4.1	0.40	1.00	0.34	0.63	0.48	0.10	0.38	0.15	0.007	
18 822-823C*	G+FT	Mdst.	S MAR	4.2	0.70	1.1	0.50	0.08	0.06	0.02	0.04	0.02	0.007	
18 822-823D*	G+FT	Mdst.	S MAR	4.0	0.34	1.1	0.15	0.63	0.42	0.04	0.42	0.16	0.01	0.5
31 263-274B*	G+FT	Slts.	NS MAR	3.8	0.22	0.31	0.52	0.25	0.74	0.03	0.20	0.01	0.01	1.6
31 263-274C	G+FT	Slts.	NS MAR	2.6	0.31	0.23	0.07	0.37	1.6	0.03	0.34	0	0.007	0
31 276	FT+G	Slts.	NS MAR	2.7	0.45	0.93	0.05	0.57	0.49	0.04	0.42	0.10	0.01	0.5
31 276A*	FT+G	Slts.	NS MAR	14.	0.32	0.75	0.11	0.63	0.83	0.24	0.38	0.01	0.007	
31 353	FT+G	Mdst.	NS MNM	1.1	0.53	1.4	0	0.47	0.17	0.02	0.22	0.21	0.02	0.7
14 700-710A*	FT	Ss.	Gr MAR	1.9	0.03	0.27	1.13	0.01	0.04	0.01	0.01	0.007	0.007	
14 700-710B*	FT	Ss.	Gr MAR	1.7	0.01	0.20	0.97	0.01	0.05	0	0.01	0.007	0.007	
26 129-130A*	FT	Slts.	NS MAR	1.6	0.33	0.75	0.19	0.38	0.51	0.02	0.36	0.007	0.007	
31 211-219*	FT	Ss.	NS MNM	2.0	0.65	0.19	0.03	0.97	4.1	0.07	0.71	0.19	0.007	
31 228B*	FT	Ss.	NS MNM	11.	0.71	0.19	2.5	0.83	4.4	0.01	0.82	0.007	0.007	
31 228C	FT	Ss.	NS MNM	2.9	0.48	0.20	2.6	0.62	2.70	0.01	0.53	0.07	0.01	3

* Denotes specimens analyzed magnetically, table 2. Values in weight percent for FeHCl, acid-soluble iron; Fe cr sol, iron solubilized in chromium solution; Organic C, organic carbon; Carb C, carbonate carbon; S, tot-sum, total sulfur, the sum of all S components; AVS, acid-volatile S; Di S, disulfide S; SO_4 S, sulfate S; S org, organic S (S in kerogen and bitumen) on a whole-rock basis; S in OM, S in organic matter based on the content of organic carbon. S/C, ratio of AVS + disulfide S to organic carbon.

TABLE 4

Averages and standard deviations of geochemical data, Cretaceous units, Simpson Peninsula, Alaska

Formation or Mag Min Group	No. Samples Mag Min Group		Fe acid	Fe cr	Organic C	Carb C	Stot-sum	S/C	AVS	Di S	SO_4 S
SEABEE	19 G & 4 G+FT	AVG	3.5	0.22	1.05	0.38	0.31	0.23	0.08	0.14	0.08
		STDS	0.98	0.15	0.29	0.19	0.19	0.15	0.05	0.14	0.05
UNDIFF	6 G & 4 FT	AVG	4.0	0.36	0.49	0.50	0.44	1.3	0.05	0.34	0.05
NINUKUK-SEABEE	2 G+FT 3 FT+G	STDS	3.6	0.21	0.41	0.85	0.27	1.4	0.06	0.23	0.07
GREIGITE	25	AVG	3.2	0.18	0.90	0.35	0.27	0.34	0.08	0.13	0.06
		STDS	0.89	0.13	0.43	0.21	0.17	0.39	0.05	0.12	0.05
GREIGITE + FT	6 G+FT 3 FT+G	AVG	4.6	0.40	0.85	0.23	0.48	0.59	0.06	0.32	0.09
		STDS	3.7	0.14	0.37	0.20	0.21	0.45	0.07	0.14	0.08
FT GROUP	6 FT	AVG	3.5	0.37	0.30	1.2	0.47	2.0	0.02	0.41	0.05
		STDS	3.8	0.30	0.22	1.1	0.41	2.0	0.03	0.34	0.07
GRANDSTAND	2 FT	AVG			0.24	1.1	0.01	0.05	0.005	0.01	0.007
		STDS			0.05	0.11	0	0.01			

AVG, average; STDS, sample standard deviation. Other abbreviations as in table 3.

the greigite-bearing, marine Seabee Formation is characterized by a narrow band in organic C (about 1.0 wt percent) and by a wide range of corresponding values of reduced sulfur, most values much lower than predicted from diagenetic S/C relations. In contrast, most samples from the undifferentiated Ninuluk and Seabee Formations have lower contents of organic carbon and higher S/C ratios. These comparisons suggest that (1) the canyon-fill Seabee represents a sulfur-limited system; and (2) reduced sulfur contents in both units were controlled by processes different from those in normal marine muds.

For all samples, the average contents of iron available for sulfidization (Fe_r = 3.8 wt percent) are much greater than the sulfidized iron (DOS_r = 0.09). Values from the undifferentiated Ninukuk and Seabee Formations are similar to those from the canyon-fill Seabee. Moreover, the amounts of AVS and disulfide S are not related to Fe_r. These observations suggest that the amount of iron in these beds did not limit the production of iron sulfide minerals. This suggestion should be tempered by recent understanding that not all the iron obtained by acid digestion is a measure of the iron available for sulfidization, at least on early diagenetic time scales (Canfield, Raiswell, and Bottrell, 1992).

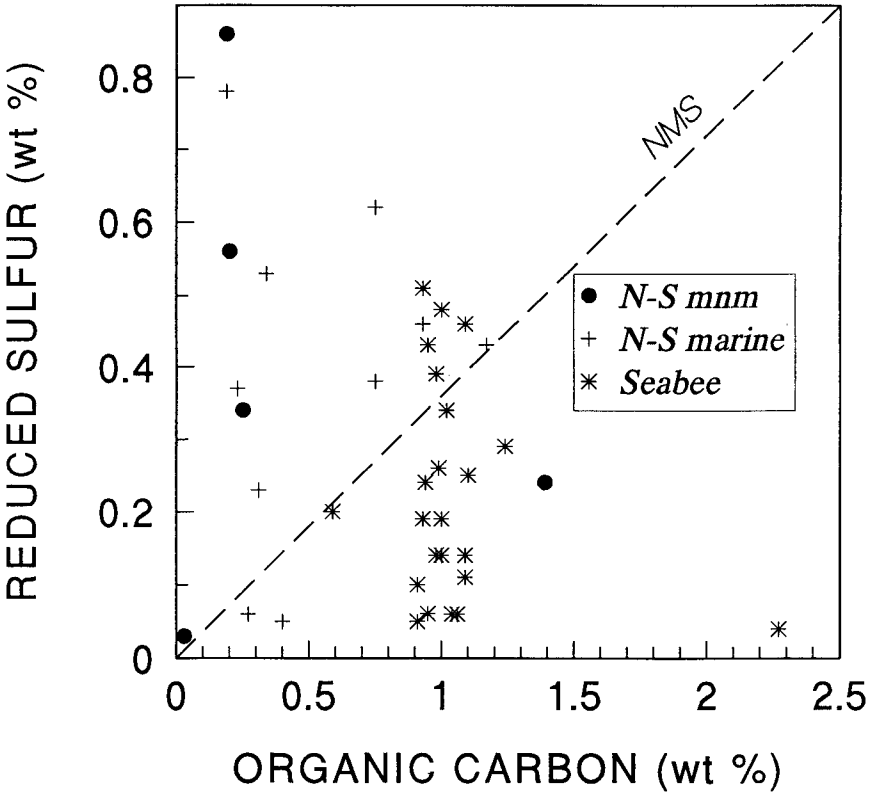

Fig. 14. Plot of reduced sulfur (the sum of disulfide and acid-volatile sulfur contents) against organic carbon. Plot is coded by formation and depositional environment. The undifferentiated Ninuluk and Seabee Formations (N-S) represent marine or indeterminate marine-nonmarine (mnm) sedimentation, whereas the Seabee Formation is entirely marine. NMS line represents a S/C ratio of 0.36, typical for normal marine sediments.

Sulfur, Carbon, and Oxygen Isotopes

Sulfur isotopic systematics can elucidate certain genetic aspects of sedimentary sulfide minerals, such as sources of sulfide and rates of sulfide reaction with iron minerals (for example, Goldhaber and Kaplan, 1980; Canfield, Raiswell, and Bottrell, 1992). Bacterial sulfate reduction (BSR) can produce sulfide having isotopic ratios enriched in light sulfur (^{32}S; $\delta^{34}S$ values typically < -20 permil) relative to the starting sulfate sulfur. As ^{32}S is depleted, the residual sulfate reservoir becomes enriched in ^{34}S.

The sulfur species in the different depositional settings have fundamentally disparate sulfur isotopic compositions (table 5; fig. 15). Disulfide sulfur and AVS in the undifferentiated Ninuluk and Seabee are variable

TABLE 5

Summary of sulfur isotopic results, Cretaceous units, Simpson Peninsula, Alaska

Formation Core	Sample	Lithology Dep Envir	Magnetic Mineral	Sample Type	$\delta^{34}S$ per mil AVS	DiS	SO_4S	S Org
GUBIK								
29	71	Ss. NM	G+FT	BULK	–		-9.1	
	83	Ss. NM	G+FT	BULK	–		-13.4	
SEABEE								
31	115	Mdst. MAR	G	MT	-19.1	-25.1	-21.1	-2.7
	115-125	Mdst. MAR	G	BULK		5.3	-19.3	
	144	Mdst. MAR	G	MT	-25.8	-29.2		
	144-155	Mdst. MAR	G	BULK		-27.5		
	166	Mdst. MAR	G	MT	-24.1	-29.2	-25.7	-5.7
	166-175A	Mdst. MAR	G	BULK		-30.2	-28.0	
	166-175B	Mdst. MAR	G	BULK		5.3	-25.6	
	175	Mdst. MAR	G	MT		-23.1	-27.3	-1.8
	175-186	Mdst. MAR	G	BULK		-23.0	-22.5	
18	204	Mdst. MAR	G	MT	-21.3	-32.2		
	408	Mdst. MAR	G	MT	-24.9	-32.4	-30.6	
	624	Mdst. MAR	G+FT	MT	-21.0	-32.0		-2.1
	624	Mdst. MAR	G+FT	BULK		-34.8	-29.2	
	822	Mdst. MAR	G+FT	MT	-18.6	-32.4	-27.7	
29	366A	Slts. MAR	G	MT	-23.9	-30.1		
13	132	Slts. MAR	G	BULK	10.3	-5.8		
UNDIFF NINULUK and SEABEE								
31	211	Ss. MAR	FT	MT	-25.9	-38.3	-28.2	
	211-215H	Ss. MAR	FT	HEAVIES		-21.3	-19.3	
	213-225	Ss. MAR	FT	BULK		3.0		
	225H	Ss. MNM	FT	HEAVIES		13.7		
	85-228	Ss. MNM	FT	BULK		34.8	11.2	
	228B	Ss. MNM	FT	MT		27.5		
	228C	Ss. MNM	FT	MT		5.5		
	252	Ss. MAR	G	MT*	25.7	17.7	17.8	9.6
	252-263	Ss. MAR	G	BULK		24.4		
	252-263M	Ss. MAR	G	MAGS	22.6	25.1		
	252-263	Ss. MAR	G	BULK		25.5		
	254B	Ss. MAR	G	MT	14.2	24.2	-0.2	
	263B	Slts. MAR	FT+G	MT		20.2		
	263C	Slts. MAR	FT+G	MT	2.5	22.5		
	263-274	Slts. MAR	FT+G	BULK		24.4		
	276	Slts. MAR	G+FT	BULK	-2.9	14.9		
	283	Mdst. MAR	G	MT	-0.4	15.6	1.3	
	283	Mdst. MAR	G	BULK		11.9	-4.0	
	290H	Mdst. MNM	G	HEAVIES		21.9		
	297-304	Mdst. MAR	G	BULK		-7.8		
	309	Slts. MAR	G	BULK		19.5		
	310	Ss. MAR	G	BULK		19.3		
	310	Ss. MAR	G	MT*	26.6	8.6	17.5	6.1
	316	Ss./OIL MNM	FT+G	MT*	10.5	5.4	8.0	4.7
	314-316	Ss./OIL MNM	FT+G	BULK		14.1		
	320	Ss. MNM	G+FT	BULK		-2.1		
	325	Ss. MNM	FT+G	BULK		-2.1		
	334	Slts. MNM	FT+G	BULK		22.4		
	351	Mdst. NM		BULK		7.0		
	353	Mdst. NM	FT+G	BULK	-1.9	-6.9	-9.0	1.0
14	285-305	Mdst. MAR	FT	BULK		-27.2		
	305-315H	Ss. MNM	FT	HEAVIES		-15.2		
	495-497H	Ss. MNM	FT+G	HEAVIES		6.0		
SIDERITE CONCRETIONS THAT CONTAIN PYRITE								
SEABEE								
13	238A	Mdst. MAR		BULK		-4.5		
23	506	Mdst. MAR		BULK		-26.7		
UNDIFF NINULUK and SEABEE								
26	317	Ss. MNM		BULK		3.1		
27	232	Slts. MAR		BULK		-11.6		
30	313	Slts. MNM		MT		-0.8		
31	85-330	Slts. MNM		BULK		5.2		

Sample type indicates treatment for analysis: bulk and heavies, whole sample and heavy mineral separate, respectively, prepared and analyzed by a commercial laboratory; MT, samples prepared and analyzed at the USGS; MT*, samples separated into sulfur species at the USGS and analyzed at the commercial laboratory.

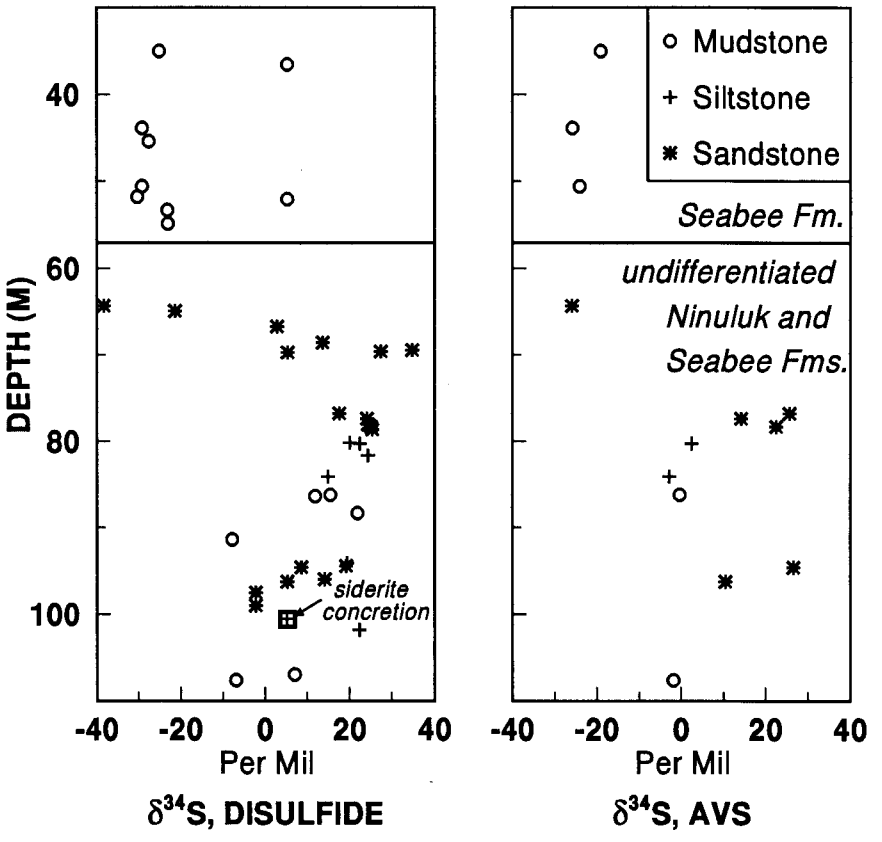

Fig. 15. Plot of $\delta^{34}S$ values from disulfide sulfur and acid-volatile sulfur (AVS) against depth in core 31. Value for pyrite in a siderite concretion is marked by a square.

($\delta^{34}S_{di}$, −38.3 to +34.8; $\delta^{34}S_{avs}$, −25.9 to +26.6 permil), and most values are positive. In contrast, all but three samples in the canyon-fill Seabee have negative values ($\delta^{34}S_{di}$, −34.8 to −23.0 permil; $\delta^{34}S_{avs}$, −25.8 to −18.6 permil) similar to those in normal marine sediments and rocks (Goldhaber and Kaplan, 1974). The exceptions are a siltstone from core 13 (sample 13-132; $\delta^{34}S_{avs}$ = 10.3 permil) and two mudstone samples from core 31 (31-115-125 and 31-166-175B; $\delta^{34}S_{di}$ = 5.3 permil). In heavy-mineral separates from the latter two samples (a separate of the sample from core 13 was not made), much of the diagenetic pyrite is cemented by pyrite and surrounded by euhedral pyritic overgrowths. Such occurrences are unlike the pyrite elsewhere in canyon-fill Seabee but similar to that in beds of the undifferentiated Ninuluk and Seabee.

Importantly, AVS in all samples of the Seabee is enriched in ^{34}S relative to coexisting disulfide sulfur by 3 to 16 permil. In the undifferen-

tiated Ninuluk and Seabee Formations, half the samples analyzed for both forms of sulfur share this relation.

Curiously, the most negative $\delta^{34}S$ value (−38.3 permil) in the study was determined for disulfide S from probable marine sandstone 7.6 m (25 ft) below the canyon-wall unconformity in core 31 (sample 31-211). Disulfide S in sandstone beneath this sample is progressively enriched in the heavy isotope with increasing depth (table 5) to a $\delta^{34}S$ value of +34.8 permil in sample 31-228 (fig. 15). Two different values (+27.5 and +5.5 permil) of disulfide S from samples within about 30 cm of sample 31-228 reflect the isotopic heterogeneity of sulfur in these sediments.

Values of $\delta^{34}S$ of the sulfate S are intermediate between the values of coexisting AVS and disulfide S. The sulfate is depleted in ^{34}S relative to Late Cretaceous marine sulfate (about +18 permil; Claypool and others, 1980), indicating that it was produced from the oxidation of the sulfide minerals.

Organosulfur (kerogen plus bitumen sulfur) in the Seabee (table 5) varies little in isotopic composition ($\delta^{34}S_{org}$ from −1.8 to −5.7 permil). These values suggest that sulfur from H_2S depleted in ^{34}S was added during diagenesis to the original assimilatory sulfur of the living organisms. Such assimilatory inherited sulfur would have had $\delta^{34}S$ values of Late Cretaceous marine sulfate (about +18 permil). The $\delta^{34}S_{org}$ in the undifferentiated Ninuluk and Seabee Formations range from +1.0 to +9.6 permil. In these beds the isotopic compositions of the H_2S and organosulfur were closer than were the sulfur types in the Seabee. The organosulfur in the bitumen fraction separated from an oil-stained sample (31-316) has a similar isotopic composition ($\delta^{34}S$ of −4.9 permil) to that of organosulfur in other oils from the Simpson area (−4 to −9 permil; Magoon and Claypool, 1981).

Pyrite in some siderite concretions may have formed during early diagenesis and thus may have $\delta^{34}S$ values characteristic of the early diagenetic sulfide in the sediments. The siderite samples, except sample 23-506, have $\delta^{13}C$ values (table 6) typical of normal marine limestone or shallow cement that thus imply an early diagenetic origin. The pyrite in the siderite from marine beds has intermediate $\delta^{34}S$ values (−11.6 and −4.5 permil; table 5). Sample 23-506, in contrast, contains isotopically heavy carbon ($\delta^{13}C$ = +12.7 permil versus PDB), pointing to diagenetic methane as a source of the carbon and isotopically light disulfide S ($\delta^{34}S$ = −26.7 permil) indicative of BSR. Three $\delta^{34}S$ values from possibly nonmarine beds range from −0.8 to 5.2 permil.

Carbon and oxygen isotopic compositions of the other carbonate phases in most samples are within the range of marine and freshwater limestones as well as shallow cements (table 6). However, several samples within a siltstone and sandstone interval in the undifferentiated Ninuluk and Seabee Formations contain carbonate minerals that are depleted in ^{13}C (−22 to −17 permil versus PDB) relative to other samples. These values imply that this carbonate formed from carbon produced by the microbial oxidation of organic matter. The presence of such carbonate,

TABLE 6

Carbon and oxygen isotopic results

Core	Sample No.	Lith	Depth (m)	$\delta^{13}C$ per mil	$\delta^{18}O$ per mil
Calcite concretions and cements					
31	175-186	Mdst.	53.3-56.7	0.7	-5.3
	190	Slts.	57.9	0.1	-4.8
	202	Ss.	61.6	25.8	-13.6
	228	Ss.	69.5	3.6	-7.9
	235	Slts.	71.6	-5.1	-17.0
	246	Slts.	75.0	-22.2	-5.3
	253	Ss.	77.1	-16.9	-5.0
	254	Ss.	77.4	-5.2	-5.9
	255-256	Ss.	77.7-80	-6.5	-6.5
	257A	Ss.	78.4	-0.1	-14.2
	257B	Ss.	78.5	-20.3	-6.1
	257D	Ss.	78.6	-19.9	-5.0
	290	Mdst.	88.4	-1.9	-13.5
	301	Mdst.	91.7	3.4	1.0
	312	Slts.	95.1	1.1	-7.3
	323	Ss.	98.5	1.3	-10.1
	324	Ss.	98.8	0.3	-14.4
	330	Ss.	100.6	-0.3	-10.5
Siderite concretions					
Seabee					
13	238A	Slts.	72.5	4.0	-7.6
23	506	Mdst.	154.2	12.7	-11.6
Undifferentiated Ninuluk and Seabee Formations					
26	317	Ss.	154.2	3.1	-8.2
27	232	Slts.	70.7	0.0	-9.5
31	330	Slts.	100.6	0.0	-10.5

with authigenic sulfide minerals may record the related microbial oxidation of organic matter and reduction of sulfate. Although the types and origins of the organic-matter substrate are not clear, as discussed below, we note that the most negative $\delta^{13}C$ values of the carbonate cement are between those values typical of the remainder of the unit (near 0 permil) and values from Simpson oils ($\delta^{13}C \approx -29$ permil versus PDB; Magoon and Claypool, 1981). A mixture of sources of carbon for the carbonate depleted in ^{13}C seems likely.

DISCUSSION

Magnetizations Carried by Greigite and Detrital Oxides

Greigite is widespread and locally abundant in Upper Cretaceous marine and nonmarine clastic rocks on the Simpson Peninsula. It also occurs in overlying Pliocene and Pleistocene beds and sporadically in

underlying Lower Cretaceous clastic rocks. The relative magnetic contribution from the greigite has been enhanced by the postdepositional destruction of detrital magnetite.

The G-group and FT-group specimens differ in some magnetic properties, such as SIRM/MS, MDI, and B_{cr} values. These differences potentially enable the recognition of a chemical remanent magnetization, carried by greigite, or detrital remanent magnetization, carried by detrital oxides, of samples for which magnetic minerals have not been independently identified. Such discrimination, however, cannot be made for specimens that contain nearly equal mixtures of the magnetic minerals. Moreover, these different magnetic characteristics may strongly reflect grain-size differences, not intrinsic magnetic properties of the different minerals. Thus, such comparisons for other sediments may not aid the distinction between greigite and Fe-Ti oxides having similar grain sizes.

Comparison of Rock Magnetic and Geochemical Results

To examine the effects of postdepositional alteration on magnetization, we compared contents of AVS and disulfide S to different magnetic-property values. The magnetic-property values, such as magnitudes of MS and NRM, of greigite-bearing specimens increase with increasing AVS contents, confirming that the AVS, or much of it, resides in greigite (fig. 16A). In contrast, contents of disulfide S have no consistent influence on magnetic properties (fig. 16B).

Origins of Greigite and Iron Disulfide Minerals

The presence of greigite, previously unreported from Cretaceous rocks, in each unit examined can be attributed to one of two possibilities: (1) greigite formed at different times in the different units, or (2) greigite formed during a single alteration event. The textural observations and sulfur isotopic data indicate that more than one generation of greigite is present. In the following sections we consider the possible origins of the iron sulfide minerals with emphasis on the sources of sulfur.

Iron sulfide minerals having sulfur depleted in ^{34}S in the canyon-fill Seabee Formation.—The negative $\delta^{34}S$ values of disulfide S in the canyon-fill Seabee are within the range of early diagenetic pyrite that forms via bacterial sulfate reduction (BSR) (Goldhaber and Kaplan, 1974). The negative $\delta^{34}S$ values result from isotopic fractionation of the source sulfate sulfur when it is reduced bacterially without appreciably depleting the sulfate reservoir (unlimited-sulfate reservoir). AVS in the same Seabee samples also had negative $\delta^{34}S$ values, strongly implying that the associated greigite is also an early diagenetic mineral. If so, it is older than any greigite yet reported.

The greigite, though, is enriched in ^{34}S with respect to the coexisting pyrite. We do not know whether this difference reflects (1) a preferential uptake of the heavy isotope relative to pyrite; (2) isotopic exchange between pore-water H_2S and AVS, but not disulfide sulfur, after burial (Tuttle, ms); or (3) the formation of greigite after pyrite as the net $\delta^{34}S$

value of the sulfate reservoir increased during progressive reduction, so that H_2S produced from it became relatively enriched in ^{34}S. In fact, a limited sulfate reservoir may partly account for the formation of the greigite: Sulfur may have been unavailable to convert the greigite to pyrite (Berner, 1981). Similar observations from modern anoxic marine sediment, in which the $\delta^{34}S$ values of AVS are greater than those of pyrite, were interpreted to indicate the formation of the AVS mineral after pyrite (Chanton, ms).

Iron sulfide minerals having sulfur enriched in ^{34}S in the undifferentiated Ninuluk and Seabee Formations.—The possible sources of the ^{34}S-enriched sulfur include (1) epigenetic aqueous sulfate solubilized from sulfate minerals in the deep, warm parts of the basin and transported in basinal fluids to the Simpson area where it was extensively reduced to sulfide by BSR; (2) epigenetic sulfide formed via thermochemical sulfate reduction (TSR) in the deep basin and similarly transported to the Simpson area; (3) epigenetic, residual sulfate derived from nearby canyon-fill Seabee and perhaps intercalated marine mud that was reduced to sulfide via BSR; and (4) early diagenetic sulfide produced by BSR from a limited sulfate reservoir. The evidence summarized below favors the first possibility. Minor contributions of sulfur described under the other possibilities may help explain the variations in the amounts and isotopic compositions of the reduced sulfur.

1. Epigenetic sulfate from basinal fluids: The North Slope basin apparently has the chemical ingredients and physical characteristics to produce and deliver aqueous sulfate to the Cretaceous rocks in the Simpson Peninsula. The basin has fluids that presumably contact sulfate minerals and that discharge in the vicinity of the Simpson area. The groundwater flow in the basin, inferred by Deming and others (1992), is topographically driven. Groundwater likely traverses fractures through the thick Brookian sequence beneath the foothills and penetrates the carbonate and clastic aquifers of the Ellesmerian sequence, some of which, such as the carbonate Lisburne Group, contain nodular anhydrite (Bird and Jordan, 1977; fig. 3). Much of the groundwater discharges above the Barrow Arch.

Another relevant aspect of the regional geology is the inference by Deming and others (1992) that variations in the thermal state of the basin have persisted for tens of millions of years, on the basis of organic maturity data. Hence, the groundwater flow system responsible for the thermal variations has probably existed over the same period (Deming and others, 1992).

The groundwater can solubilize mineral sulfate to produce aqueous sulfate which retains the sulfur isotopic composition of the original mineral. Thus aqueous sulfate derived from Carboniferous strata would have isotopic compositions about +13 to +16 permil (Claypool and others, 1980). This range is similar to that (+10 to +18 permil) in Permian to Turonian strata. If such extrinsic sulfate were the source of the ^{34}S-enriched pyrite and greigite, it was probably reduced in situ by

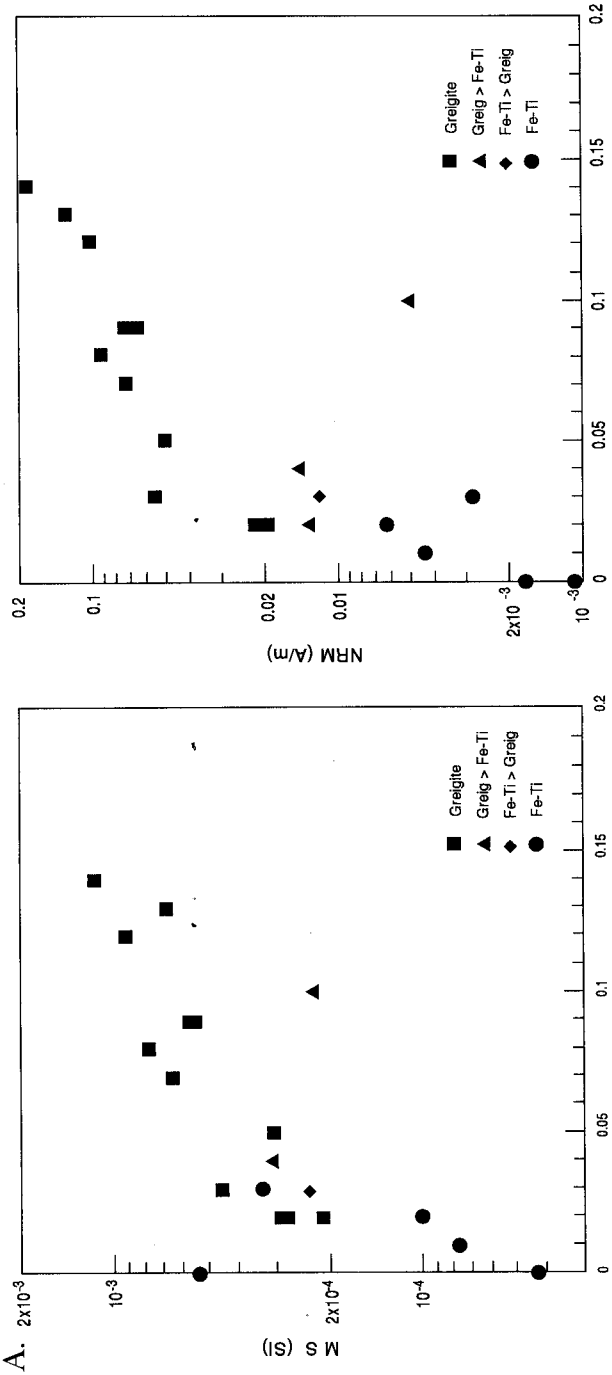
A.
M S (SI)
2x10-3
10-3
2x10-4
10-4
0
0.05
0.1
0.15
0.2
ACID-VOLATILE SULFUR (wt %)
Sulfur in greigite
Greigite
Greig > Fe-Ti
Fe-Ti > Greig
Fe-Ti
NRM (A/m)
0.2
0.1
0.02
0.01
2x10-3
10-3
0
0.05
0.1
0.15
0.2
ACID-VOLATILE SULFUR (wt %)
Sulfur in greigite
Greigite
Greig > Fe-Ti
Fe-Ti > Greig
Fe-Ti

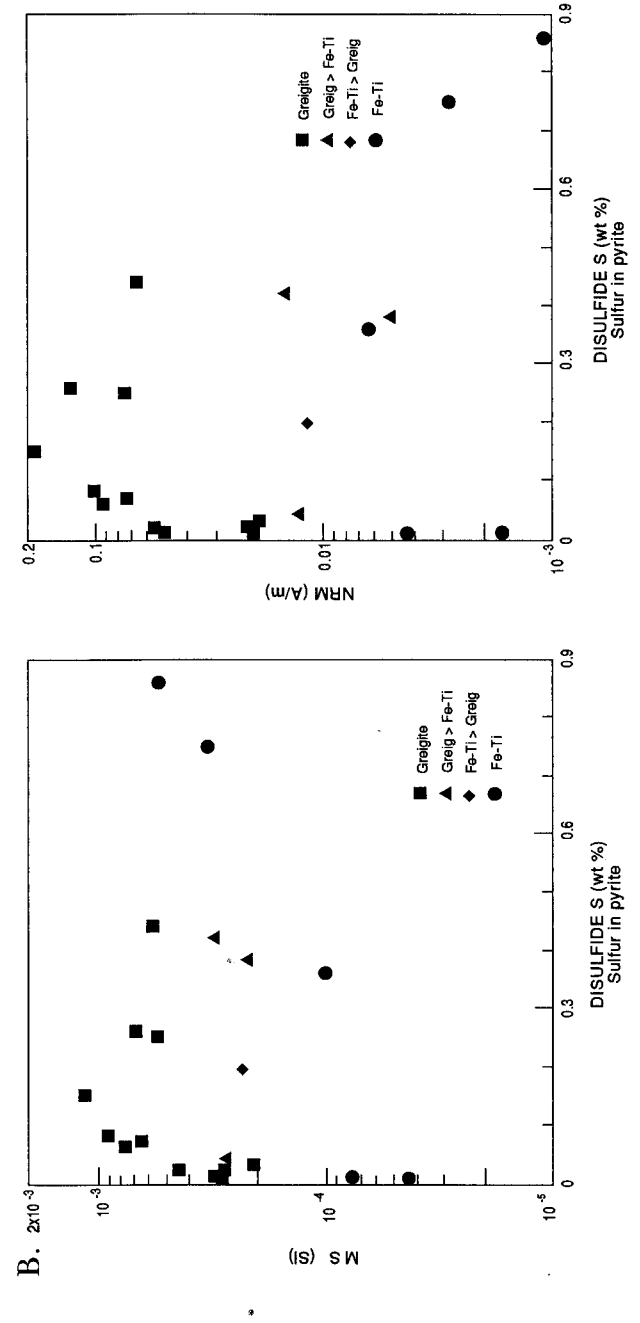

Fig. 16. Plots of magnetic susceptibility (MS) and natural remanent magnetization (NRM) against acid-volatile sulfur (A) and disulfide sulfur (B) contents. Regression analysis of acid-volatile sulfur and MS (or NRM) for specimens that contain greigite as the only magnetic mineral (squares) gives an R^2 coefficient of 0.79 (or 0.87). The positive correspondences between magnetic property values and acid-volatile sulfur (AVS) indicate that at least a high proportion of the AVS in these beds resides in magnetic minerals.

BSR, primarily in an environment that was limited in sulfate over time, to account for the even more positive $\delta^{34}S$ values (many exceed +20 permil) of the iron sulfide minerals. An unlimited supply of sulfate available for BSR would have produced sulfide minerals having very light isotopic values. BSR of extrinsic sulfate, if it occurred during migration before introduction into the beds, would also enrich the available sulfate reservoir in ^{34}S. A likely food source for sulfate-reducing bacteria under these conditions would be hydrocarbons and related compounds (see Oehler and Sternberg, 1984; Machel, 1987) in fluids that are perhaps associated with those carrying the aqueous sulfate. Along these lines, Howell and others (1992) note that North Slope oil and basinal groundwater apparently migrate along the same general pathways. Moreover, oil from reservoirs in sulfate-mineral-bearing formations far south of the Simpson Peninsula has been geochemically linked to the oil at Simpson field (Magoon and Claypool, 1988). The lack of greigite associated with the detrital plant matter in these beds suggests that such organic matter was not an easily available source of nutrients when the ^{34}S-enriched sulfide was produced via BSR.

2. Sulfide from thermochemical sulfate reduction: Aqueous sulfide as H_2S or HS^- may be produced at high temperature (above about 100°C) by the reaction of hydrocarbons or other reducing agents with sulfate minerals. As with solubilized sulfate, sulfide formed via TSR would inherit the isotopic composition of the host sulfate minerals (Orr, 1977; Goldhaber, Reynolds, and Rye, 1978; 1983; Goldhaber and Reynolds, 1991).

Although aqueous sulfide produced via TSR is a possible source of epigenetic sulfur at Simpson, it is an unlikely major source for two reasons. First, such sulfide likely would have reacted with iron over the long distances of transport, as much as 100 km. Second, the isotopic data do not favor a contribution; BSR under sulfate-limited conditions is required in this setting to generate sulfur isotopic compositions that are more positive than the sulfate values of any unit in the basin (see Claypool and others, 1980).

The one geochemical analysis of formation water in the Simpson area that bears on the sources of extrinsic sulfur does not support TSR. The sample, from Simpson Test Well 2 at 2181 to 2195 m in the Late Devonian to Early Permian (?) Endicott Group, has oxygen and deuterium isotopic compositions indicative of a meteoric origin, contains sulfate (34 mg/L SO_4), and lacks H_2S (Kharaka and Carothers, 1988).

3. Sulfate from canyon-fill Seabee Formation: Another possible source for extrinsic sulfate is from the canyon-fill Seabee. Shortly after deposition, pore-water sulfate in the Seabee may have been expelled by compaction into adjacent permeable beds of the undifferentiated Ninuluk and Seabee where the sulfate was reduced by BSR. If so, the requisite bacterial food sources are conjectural and include: (1) hydrocarbons; (2) detrital organic debris within the undifferentiated Ninuluk and Seabee rocks; or (3) organic matter, perhaps as soluble organic compounds, flushed with the sulfate from the Seabee into the adjacent beds. We have no indepen-

dent clues to elucidate the types and origins of the bacterial food source under this possibility.

A source of sulfate from the Seabee Formation may help explain the apparent trend of very negative $\delta^{34}S$ values at the top of the undifferentiated Ninuluk and Seabee sequence in core 31 which change systematically to positive values over a depth from 65.5 to 69.5 m (215-228 ft). This interpretation is weakened, however, by the presence of isotopically positive sulfur ($\delta^{34}S_{di} \approx +5$ permil) and coarse-grained iron disulfide minerals around fine-grained pyrite, as commonly seen in the undifferentiated Ninuluk and Seabee, in a few samples from the canyon-fill Seabee in core 31 (table 5). These results suggest that some sulfur was added locally to the Seabee by extrinsic fluids, as it was added to the undifferentiated Ninuluk and Seabee Formations, perhaps along fractures that tapped the Ninuluk and Seabee.

4. Early diagenetic iron sulfide: Finally, the possibility that early diagenetic BSR produced the ^{34}S-enriched sulfur under sulfate-limited conditions fails in view of the locally high contents of reduced sulfur (table 3) as well as petrographic evidence for a later generation of sulfide minerals. Together these observations suggest the addition of sulfur into the undifferentiated Ninuluk and Seabee rocks. Nevertheless, small amounts of early diagenetic sulfide enriched in ^{34}S may contribute to the isotopic signature of some nonmarine samples.

Iron sulfide minerals having negative and intermediate $\delta^{34}S$ values in the undifferentiated Ninuluk and Seabee Formations.—The few very negative $\delta^{34}S$ values (less than -20 permil) for AVS or disulfide S in the beds outside the canyon are interpreted to have formed during early diagenesis via BSR. The intermediate $\delta^{34}S$ values (between -20 and $+20$ permil) may reflect a component of early diagenetic sulfide masked to varying degrees by epigenetic sulfide further enriched in ^{34}S. This interpretation is supported by petrographic observations of framboidal pyrite and other fine-grained forms along with paragenetically later pyrite in the same samples.

The sulfur isotopic compositions of fine-grained pyrite in siderite are consistent with, but do not refine, the above interpretations. If the intermediate $\delta^{34}S$ values (-11.6 to 5.2 permil) from the undifferentiated Ninuluk and Seabee Formations represent early diagenetic sulfide, then the more positive values for pyrite and greigite through the bulk of the sediment represent a different, and presumably later, generation of sulfide.

Preservation of Greigite

The preservation of early diagenetic greigite in the Seabee Formation is a conundrum, because greigite is considered to be metastable with respect to pyrite. Greigite converts to pyrite in the presence of HS^- at concentrations above pyrite saturation and an oxidizing agent (Berner, 1970, 1981, 1984; Morse and others, 1987). In general, the factors that determine the production of pyrite and monosulfide in sediments are: (1)

the availability of organic matter that can be metabolized by sulfate-reducing bacteria; (2) the concentration of sulfate in the sediment; (3) the concentration and reactivity of iron minerals; and (4) the production of elemental sulfur via bacterial oxidation of H_2S (Berner, 1970, 1974, 1978, 1984; Canfield and Raiswell, 1991). Greigite preservation would be favored in sediments having low concentrations of dissolved sulfate and (or) in those deposited rapidly. Rapid deposition may limit the availability of sulfate by increasing the length of the path for sulfate diffusion. For example, factors such as dilution by high freshwater runoff and extraordinarily high sedimentation rates related to possible slumping in the Simpson Canyon would have favored the preservation of greigite. We have no independent evidence for low sulfate contents in the initial Seabee pore waters or for a high sedimentation rate in the submarine canyon.

Amounts of sulfur alone as the factor controlling greigite preservation in the undifferentiated Ninuluk and Seabee Formations, however, cannot explain the observation that greigite is abundant in many samples regardless of sulfur contents. In this setting, the epigenetic production of greigite may be tied to the rate of sulfate flux in groundwater and the redox conditions of alteration.

Comparison of the results from the Seabee to those from other Late Cretaceous marine shales of the Western Interior Seaway (WIS) of North America (Gautier, 1986, 1987; Dean and Arthur, 1989) may elucidate the conditions that favor the presence of early diagenetic greigite. The Seabee rocks may differ in some chemical respects from many WIS shale units, because the Seabee muds were deposited—perhaps rapidly—near the coast far to the north of the other units, at the edge of the Seaway (Kauffman, 1984). As an example, changes in the chemical and physical conditions of seawater, such as salinity, oxygen contents, and temperature, may have led to different amounts and types of organic matter and different fluxes of sulfate in the different depositional settings along and across the seaway.

Although detailed comparisons among formations are not made here, differences in S/C ratios and amounts of organic carbon may reflect some fundamentally different paleoenvironmental factors. The Seabee samples have a low S/C ratio (0.23) with a relatively low content of organic carbon (about 1 wt percent). In contrast, samples from the Upper Cretaceous shales of the WIS have an average S/C ratio of about 0.67, and most samples contain more than 1 percent organic carbon (Gautier, 1986). The average global value for normal marine Upper Cretaceous shales is ≈ 0.5, and the data show considerable dispersion (Raiswell and Berner, 1986; Dean and Arthur, 1989). The relatively high S/C and organic carbon values in the shales of the Seaway have been attributed to related factors of low levels of oxygen, restricted circulation, limited bioturbation, and low sedimentation rates (Gautier, 1986).

The above comparisons, however, should be considered cautiously. In the studies cited above, analytical methods were different from the ones used in our study and were not designed to test for the presence of greigite. Thus, we cannot be certain that the differences in S/C ratios among the different sample suites are related to the presence or absence of greigite or are caused by different paleoenvironmental factors.

Nevertheless, the chemical relations identified herein for beds that contain early diagenetic greigite may help target other Cretaceous sediments that might also contain such greigite. Further work would evaluate early diagenetic greigite, if found elsewhere, as an indicator of environmental conditions, such as sedimentation rate, temperature, salinity, and oxygen content in bottom waters.

The preservation of greigite in stored cores for more than 40 yrs is also noteworthy. Some of the changes in magnetic properties of some soft sediment cores measured only days or weeks after collection result from oxidation of greigite (Hilton, 1990). Although some of the greigite originally in the Simpson cores may have been altered to minerals of lesser magnetization during initial drying or during later handling, we found no evidence for such loss of greigite, other than perhaps the sporadic presence of sulfate.

SOURCES OF MAGNETIC ANOMALIES

Greigite is most likely the main source for aeromagnetic anomalies at Simpson, on the basis of its widespread occurrence and high magnetizations. Another possible source for the magnetic contrast is detrital magnetite that may be concentrated in channel sands of the Gubik Formation. Sufficient samples to evaluate such a source have not been obtained. Nevertheless, the thicknesses of sand of the Gubik (Robinson, 1964) do not correspond to magnetic anomalies and thus do not support this possibility. Siderite is not a viable magnetic source, because it is extremely rare.

A difficulty in evaluating the magnetic sources at Simpson field is the lack of oriented samples with which to determine the directions of NRM whose magnitudes overwhelm those of induced magnetizations. High Koenigsberger ratios (table 2, Q, 1-5) in greigite-bearing samples underscore the potential importance of remanent magnetization in this setting.

Greigite, if formed during diagenetic alteration within a few hundreds to even a few millions of years after deposition, probably carries normal directions. This is because the age span of the Ninuluk and Seabee Formations (about 97-88 Ma) falls within the 124- to 83-Ma interval of constant normal polarity during Cretaceous time (Harland and others, 1990). On the other hand, if the epigenetic greigite formed at nearly constant rates over much of Cenozoic time and not mainly over the past 780,000 yrs of normal polarity, it would carry nearly equal proportions of normal and reversed chemical magnetizations, thereby canceling the effect of remanence. Perhaps the anomaly is related to

magnetic contrasts caused by the juxtaposition of greigite-bearing beds having total magnetizations dominated by Cretaceous normal remanent magnetizations against greigite-bearing beds having total magnetizations that are subdued by the presence of normal and reversed polarities.

SUMMARY

The geochemical, isotopic, and petrographic results imply that two different generations of iron disulfide minerals and greigite have formed in the Cretaceous beds under much different conditions: (1) in the Seabee Formation, early diagenetic iron sulfide formed via BSR involving pore-water sulfate; and (2) in the undifferentiated Ninuluk and Seabee Formations, iron sulfide formed via BSR involving epigenetic sulfate, perhaps from basinal fluids, and epigenetic organic matter, perhaps hydrocarbons. BSR under sulfate-limited conditions is the most plausible explanation for the ^{34}S-enriched sulfide in the iron disulfide and greigite in the undifferentiated Ninuluk and Seabee. Possibly, the sulfate was added slowly over a long period of time, so that the system at any moment may have been effectively sulfate-limited with respect to metabolizable organic matter.

The conditions responsible for the ^{34}S-enriched sulfide in the undifferentiated Ninuluk and Seabee locally affected canyon-fill Seabee. Basinal fluids that carry sulfate and possibly hydrocarbons through the permeable beds of the Ninuluk and Seabee may have penetrated the Seabee along fractures. The presence of greigite in the Pliocene and Pleistocene Gubik Formation that caps the Cretaceous beds may provide another clue to the origin of the greigite in the undifferentiated Ninuluk and Seabee Formations. Greigite may be forming today as fluids continue to move through permeable beds and along fractures in the permafrost.

ACKNOWLEDGMENTS

We thank Marty Goldhaber and Ken Bird for helpful discussions; Don Gautier, Don Canfield, Bob Karlin, and John King for reviewing the manuscript; and Doc Atkinson for help with sampling. This work was supported by the Evolution of Sedimentary Basins Program and the Onshore Oil and Gas Program of the U.S. Geological Survey.

REFERENCES

Banerjee, S. K., King, J., and Marvin, J., 1981, A rapid method for magnetic granulometry with applications to environmental studies: Geophysical Research Letters, v. 8, p. 333–336.

Berner, R. A., 1970, Sedimentary pyrite formation: American Journal of Science, v. 268, p. 1–23.

———— 1974, Iron sulphides in Pleistocene deep Black Sea sediments and their paleooceanographic significance, *in* Degens, E. T., and Ross, D. A., editors, The Black Sea—Geology, Chemistry, Biology: American Association of Petroleum Geologists Memoir 20, p. 523–531.

———— 1978, Sulfate reduction and the rate of deposition of marine sediments: Earth and Planetary Science Letters, v. 37, p. 492–498.

———— 1981, Authigenic mineral formation resulting from organic matter decomposition in modern sediments: Fortschritte der mineralogie, v. 59, p. 117–135.

———— 1984, Sedimentary pyrite formation: An update: Geochimica et Cosmochimica Acta, v. 48, p. 605–615.

Bird, K. J., 1987, The framework geology of the north slope of Alaska as related to oil-source correlations, *in* Tailleur, I. and Weimer, P., editors, Alaskan North Slope Geology, v. 1: Bakersfield, California, Society of Economic Paleontologists and Mineralogists, Pacific section, p. 121–141.

———— 1988, Structure-contour and isopach maps of the National Petroleum Reserve in Alaska, *in* Gryc, G., editor, Geology and exploration of the National Petroleum Reserve in Alaska, 1974–1982: U.S. Geological Survey Professional Paper 1399, p. 355–377.

———— 1991, North slope of Alaska, *in* Gluskoter, H. J., Rice, D. D., and Taylor, R. B., editors, Economic Geology, U.S., Oil and Gas Section, Part III, Regional synthesis of selected provinces, chapter 29: Boulder, Colorado, Geological Society of America, The geology of North America, DNAG Series v. P-2, p. 447–462.

Bird, K. J., and Jordan, C. F., 1977, Lisburne Group (Mississippian and Pennsylvanian), potential major hydrocarbon objective of arctic slope, Alaska: American Association of Petroleum Geologists Bulletin, v. 61, p. 1493–1512.

Boardman, J. W., 1987, Modelling of oilfield equipment on low altitude magnetic surveys, *in* Proceedings of the Fifth Thematic Conference on Remote Sensing for Exploration Geology; Technology for a competitive world, v. 1: Environmental Research Institute of Michigan, p. 249–261.

Bonev, I. K., Khrischev, K. G., Neikov, H. N., and Georgiev, V. M., 1989, Mackinawite and greigite in iron sulphide concretions from Black Sea sedments: Comptes Rendus de l'Academie Bulgare des Sciences, v. 42, p. 97–100.

Brandsma, D., Lund, S. P., and Henyey, T. L., 1989, Paleomagnetism of late Quaternary marine sediments from Santa Catalina basin, California continental borderland: Journal of Geophysical Research, v. 94, p. 547–564.

Butler, R. F., and Lindsay, E. H., 1985, Mineralogy of magnetic minerals and revised magnetic polarity stratigraphy of continental sediments, San Juan basin, New Mexico: Journal of Geology, v. 93, p. 535–554.

Canfield, D. E., and Berner, R. A., 1987, Dissolution and pyritization of magnetite in anoxic marine sediments: Geochimica et Cosmochimica Acta, v. 51, p. 645–659.

Canfield, D. E., and Raiswell, R., 1991, Pyrite formation and fossil preservation, *in* Allison, P., and Briggs, D. E., Taphonomy, releasing the information locked in the fossil record: New York, Plenum Press, p. 337–387.

Canfield, D. E., Raiswell, R., and Bottrell, S., 1992, The reactivity of sedimentary iron minerals toward sulfide: American Journal of Science, v. 292, p. 659–683.

Channell, J. E. T., and Hawthorne, T., 1990, Progressive dissolution of titanomagnetites at ODP site 653 (Tyrrhenian Sea): Earth and Planetary Science Letters, v. 96, p. 469–480.

Chanton, J. P., ms, 1985, Sulfur mass balance and isotopic fractionation in an anoxic marine sediment: Ph.D. thesis, University of North Carolina, Chapel Hill.

Chanton, J. P., and Martens, C. S., 1985, The effects of heat and stannous chloride addition on the active distillation of acid-volatile sulfide from pyrite-rich marine sediment samples: Biogeochemistry, v. 1, p. 375–383.

Clark, D. A., 1983, Comments on magnetic petrophysics: Australian Society Exploration Geophysics Bulletin, v. 4, p. 49–62.

Claypool, G. E., Holser, W. T., Kaplan, I. R., Sakai, H., and Zak, I., 1980, The age curves of sulfur and oxygen isotopes in marine sulfate and their mutual interpretation: Chemical Geology, v. 28, p. 199–260.

Cornwell, J. C., and Morse, J. W., 1987, The characterization of iron sulfide minerals in anoxic marine sediments: Marine Chemistry, v. 22, p. 193–206.

Cutter, G. A., and Velinsky, D. J., 1988, Temporal variations of sedimentary sulfur in a Delaware salt marsh: Marine Chemistry, v. 23, p. 311–327.

Dean, W. E., and Arthur, M. A., 1989, Iron-sulfur-carbon relationships in organic-carbon-rich sequences I: Cretaceous western interior seaway: American Journal of Science, v. 289, p. 708–743.

Dell, C. I., 1972, An occurrence of greigite in Lake Superior sediments: American Mineralogist, v. 57, p. 1303–1304.

Deming, D., Sass, J. H., Lachenbruch, A. H., and DeRito, R. F., 1992, Heat flow and subsurface temperature as evidence for basin-scale groundwater flow, North Slope of Alaska: Geological Society of America Bulletin, v. 104, p. 528–542.

Demitrack, A., 1985, A search for bacterial magnetite in the sediments of Eel Marsh, Woods Hole, Massachusetts, *in* J. Kirschvink, J. L., Jones, D. S., and McFadden, B. J., editors, Magnetite biomineralization and magnetoreception in organisms: New York, Plenum Press, p. 626–645.

Donovan, T. J., Hendricks, J. D., Roberts, A. A., and Eliason, P. T., 1988, Low-level aeromagnetic surveying for petroleum in arctic Alaska, *in,* Gryc, G., editor, Geology and exploration of the National Petroleum Reserve in Alaska, 1974–1982: U.S. Geological Survey Professional Paper 1399, v. 1, p. 623–632.

Freeman, R., Heller, F., and Rogenmoser, G., 1983, A stable reversed remanence carried by greigite in Pliocene marls from Balerna, Switzerland: International Union of Geodesy and Geophysics, 28th, Hamburg, International Association of Geophysics and Aeronomy abstracts volume, p. 209.

Frischknecht, F. C., Grette, R., Raab, P. V., and Meredith, J., 1985, Location of abandoned wells by magnetic surveys: Acquisition and interpretation of aeromagnetic data for five test areas: U.S. Geological Survey Open-file Report 85-614A, 654 p.

Gautier, D. L., 1986, Cretaceous shales from the western interior of North America: Sulfur/carbon ratios and sulfur-isotope composition: Geology, v. 14, p. 225–228.

———— 1987, Isotopic composition of pyrite: relationship to organic matter type and iron availability in some North American Cretaceous shales: Chemical Geology, v. 65, p. 293–303.

Giovanoli, F., 1979, A comparison of the magnetization of detrital and chemical sediments from Lake Zurich: Geophysical Research Letters, v. 6, p. 233–235.

Goldhaber, M. B., and Kaplan, I. R., 1974, The sulfur cycle, *in* Goldberg, E. D., editor, The Sea: Marine Chemistry, 5, p. 569–655.

———— 1980, Mechanisms of sulfur incorporation and isotopic fractionation during early diagenesis in sediments of the Gulf of California: Marine Chemistry, v. 9, p. 95–143.

Goldhaber, M. B., and Reynolds, R. L., 1991, Relations among hydrocarbon reservoirs, epigenetic sulfidization, and rock magnetization: Examples from the south Texas coastal plain: Geophysics, v. 56, p. 748–757.

Goldhaber, M. B., Reynolds, R. L., and Rye, R. O., 1978, The origin of a south Texas roll-type uranium deposit: II. Sulfide petrology and sulfur isotope studies: Economic Geology, v. 73, p. 1690–1705.

———— 1983, Role of fluid mixing and fault-related sulfide in the origin of the Ray Point uranium district, south Texas: Economic Geology, v. 78, p. 1043–1063.

Gryc, G., editor, 1988, Geology and exploration of the National Petroleum Reserve in Alaska, 1974 to 1982: U.S. Geological Survey Professional Paper 1399, 940 p.

Harland, W. B., Armstrong, R. L., Cox, A. V., Craig, L. E., Smith, A. G., and Smith, D. G., 1990, A Geologic Time Scale 1989: New York, Cambridge University Press, 263 p.

Henshaw, P. C., and Merrill, R. T., 1980, Magnetic and chemical changes in marine sediments: Reviews of Geophysics and Space Physics, v. 18, p. 483–504.

Hilton, J., 1990, Greigite and the magnetic properties of sediments: Limnology and Oceanography, v. 35, p. 509–520.

Hoffmann, V., 1992, Greigite (Fe_3S_4): magnetic properties and first domain observations: Physics of the Earth and Planetary Interiors, v. 70, p. 288–301.

Horng, C. S., Tric, E., Cadoret, C., Jehanno, C., Laj, C. Lee, T. Q., and Kissel, C., 1989, Widespread presence of greigite in Plio-Pleistocene marine marls from northern Italy and Taiwan: EOS (Transactions of the American Geophysical Union), v. 70, p. 1066.

Howell, D. G., Bird, K. J., Huafu, L., and Johnsson, M. J., 1992, Tectonics and petroleum potential of the Brooks Range fold and thrust belt—a progress report, *in* Bradley, D. C., and Ford, A. B., Geologic studies in Alaska by the U.S. Geological Survey, 1990: U.S. Geological Survey Bulletin 1999, p. 112–126.

Jedwab, J., 1967, Minéralisation en greigite de débris végétaux d'une vase récente (Grote Geul): Bulletin de la Société Belge de Géologie de Paléontologie et d'Hydrologie, v. 76, p. 27–38.

Kalcheva, V., Nozharov, P., Kovasheva, M., and Shopov, V., 1990, Paleomagnetic research on Black Sea Quaternary sediments: Physics of the Earth and Planetary Interiors, v. 63, p. 113–120.

Karlin, R., 1990a, Magnetite diagenesis in marine sediments from the Oregon continental margin: Journal of Geophysical Research, v. 95, p. 4405–4419.

———— 1990b, Magnetic mineral diagenesis in suboxic sediments at Bettis site W-N, NE Pacific Ocean: Journal of Geophysical Research, v. 95, p. 4421–4436.

Karlin, R., and Levi, S., 1985, Geochemical and sedimentological control of the magnetic properties of hemipelagic sediments: Journal of Geophysical Research, v. 90, p. 10,373–10,392.

Kauffman, E. G., 1984, Paleobiogeography and evolutionary response dynamic in the Cretaceous Western Interior Seaway of North America, *in* Westermann G. E. G., editor, Jurassic-Cretaceous Biochronology and Paleogeography of North America: Geological Association of Canada Special Paper 27, p. 272–306.

Kharaka, Y. K., and Carothers, W. W., 1988, Geochemistry of oil-field water from the north slope, *in* Gryc, G., editor. Geology and exploration of the National Petroleum Reserve in Alaska, 1974–1982: U.S. Geological Survey Professional Paper 1399, v. 1, p. 551–561.

Krs, M., Krsová, M., Pruner, P., Zeman, A., Novák, F., and Jansa, J., 1990, A petromagnetic study of Miocene rocks bearing micro-organic material and the magnetic mineral greigite (Sokolov and Cheb basins, Czechoslovakia): Physics of the Earth and Planetary Interiors, v. 63, p. 98–112.

Krs, M., Novák, F., Krsová, M., Pruner, P., Kouklíková, L., and Jansa, J., 1992, Magnetic properties and metastability of greigite-smythite mineralization in brown-coal basins of the Krusné hory Piedmont, Bohemia: Physics of the Earth and Planetary Interiors, v. 70, p. 273–287.

Larson, E. E., Patterson, P. E., and Evanoff, E., 1990, The engimatic occurrence of hemo-ilmenite in Tertiary basin-fill strata in northern and central Wyoming: EOS (Transactions of the American Geophysical Union), v. 71, p. 1288.

Leslie, B. W., Hammond, D. E., Burleson, W. M., and Lund, S. P., 1990, Diagenesis in anoxic sediments from the California continental borderland and its influence on iron, sulfur, and magnetite behavior: Journal of Geophysical Research, v. 95, p. 4453–4470.

Leslie, B. W., Lund, S. P., and Hammond, D. E., 1990, Rock magnetic evidence for dissolution and authigenic growth of magnetic minerals within anoxic marine sediments of the California continental borderland: Journal of Geophysical Research, v. 95, p. 4437–4452.

Lin, S., and Morse, J. W., 1991, Sulfate reduction and iron sulfide mineral formation in Gulf of Mexico anoxic sediments: American Journal of Science, v. 291, p. 55–89.

Machel, H. G., 1987, Some aspects of diagenetic sulphate-hydrocarbon redox reactions, *in* Marshall, J. D., editor, Diagenesis of Sedimentary Sequences: Geological Society London Special Publication 36, p. 15–28.

Magoon, L. B., and Claypool, G. E., 1981, Two oil types on north slope of Alaska—implications for exploration: American Association of Petroleum Geologists Bulletin, v. 65, p. 644–652.

———— 1988, Geochemistry of oil occurrences, National Petroleum Reserve in Alaska, *in* Gryc, G., editor, Geology and exploration of the National Petroleum Reserve in Alaska, 1974–1982: U.S. Geological Survey Professional Paper 1399, v. 1, p. 519–549.

Mann, S., Sparks, N. H. C., Frankel, R. B., Bazylinski, D. A., and Jannasch, H. W., 1990, Biomineralization of ferrimagnetic greigite (Fe_3S_4) and iron pyrite (FeS_2) in a magnetotactic bacterium: Nature, v. 343, no. 6255, p. 258–261.

Molenaar, C. M., 1983, Depositional relations of Cretaceous and lower Tertiary rocks, northeastern Alaska: American Association of Petroleum Geologists Bulletin, v. 67, p. 1066–1080.

Morse, J. W., and Cornwell, J. C., 1987, Analysis and distribution of iron sulfide minerals in recent anoxic marine sediments: Marine Chemistry, v. 22, p. 55–69.

Morse, J. W., Millero, F. J., Cornwell, J. C., and Rickard, D. T., 1987, The chemistry of the hydrogen sulfide and iron sulfide systems in natural waters: Earth-Science Reviews, v. 24, p. 1–42.

Nagata, T., and Akimoto, A., 1956, Magnetic properties of ferromagnetic ilmenites: Geofisica Pura E Applicata, v. 34, p. 36–50.

Oehler, D. Z., and Sternberg, 1984, See page-induced anomalies, "false" anomalies, and implications for electrical prospecting: American Association for Petroleum Geologists Bulletin, v. 68, p. 1121–1145.

Orr, W. L., 1977, Geologic and geochemical controls on the distribution of hydrogen sulfide in natural gas, *in* Campos, R., and Goni, J., editors, Advances in Organic Geochemistry: Madrid, Spain, Enadisma, p. 571–597.

Petersen, N., Von Dobonek, T., and Vali, H., 1986, Fossil bacterial magnetite in deep-sea sediments from the South Atlantic Ocean: Nature, v. 320, p. 611–615.

Pye, K., 1981, Marshrock formed by iron sulphide and siderite cementation in saltmarsh sediments: Nature, v. 294, p. 650–652.

Raiswell, R., and Berner, R. A., 1986, Pyrite and organic matter in Phanerozoic normal marine shales: Geochimica et Cosmochimica Acta, v. 50, p. 1967–1976.

Reynolds, R. L., 1977, Magnetic titanohematite minerals in uranium-bearing sandstones: U.S. Geological Survey Open-file Report, 77–355, 21 p.

———— 1982, Postdepositional alteration of titanomagnetite in a Miocene sandstone, south Texas (U.S.A.): Earth and Planetary Science Letters, v. 61, p. 381–391.

Reynolds, R. L., Fishman, N. S., and Hudson, M. R., 1991, Sources of aeromagnetic anomalies over Cement oil field (Oklahoma), Simpson oil field (Alaska), and the Wyoming-Idaho-Utah thrust belt: Geophysics, v. 56, p. 606–617.

Reynolds, R. L., Fishman, N. S., Wanty, R. B., and Goldhaber, M. B., 1990, Iron sulfide minerals at Cement oil field, Oklahoma: Implications for magnetic detection of oil fields: Geological Society America Bulletin, v. 102, p. 368–380.

Rice, C. A., Tuttle, M. L., and Reynolds, R. L., 1993, The analysis of forms of sulfur in ancient sediments and sedimentary rock: Comments and cautions: Chemical Geology, v. 107, p. 83–95.

Roberts, A. P., and Turner, G. M., 1993, Diagenetic formation of ferrimagnetic iron sulphide minerals in rapidly deposited marine sediments, South Island, New Zealand: Earth and Planetary Science Letters, v. 115, p. 257–273.

Robinson, F. M., 1964, Core tests Simpson area, Alaska: U.S. Geological Survey Professional Paper 305-L, p. 645–730.

Schwarz, E. J., 1974, Magnetic properties of pyrrhotite and their use in applied geology and geophysics: Geological Survey of Canada Paper 74–59, 24 p.

Sherman, D. M., 1990, Mössbauer spectra, crystal chemistry, and electronic structure of greigite, Fe_3S_4: EOS (Transactions American Geophysical Union), v. 71, p. 1649.

Skinner, B. J., Erd, R. C., and Grimaldi, F. S., 1964, Greigite, the thio-spinel of iron; a new mineral: American Mineralogist, v. 49, p. 543–555.

Snowball, I. F., 1991, Magnetic hysteresis properties of greigite (Fe_3S_4) and a new occurrence in Holocene sediments from Swedish Lappland: Physics of the Earth and Planetary Interiors, v. 68, p. 32–40.

Snowball, I. F., and Thompson, R., 1990a, A mineral magnetic study of Holocene sedimentation in Lough Catherine, Northern Ireland: Boreas, v. 19, p. 127–146.

———— 1990b, A stable chemical remanence in Holocene sediments: Journal of Geophysical Research, v. 95, p. 4471–4479.

Spender, M. R., Coey, M. D., and Morrish, A. H., 1972, The magnetic properties and Mössbauer spectra of synthetic samples of Fe_3S_4: Canadian Journal Physics, v. 50, p. 2313–2326.

Suthill, R. J., Turner, P., and Vaughan, D. J., 1982, The geochemistry of iron in Recent tidal flat sediments of the Wash area, England: a mineralogic, Mössbauer, and magnetic study: Geochimica et Cosmochimica Acta, v. 46, p. 205–217.

Sweeney, R. E., and Kaplan, I. R., 1973, Pyrite framboid formation: Laboratory synthesis and marine sediments: Economic Geology, v. 68, p. 618–634.

———— 1980, Diagenetic sulfate reduction in marine sediments: Marine Chemistry, v. 9, p. 165–174.

Tailleur, I., and Weimer, P., eds., 1987, Alaskan North Slope Geology, v. 1: Bakersfield, California, Society of Economic Paleontologists and Mineralogists, Pacific section, Book 50, 874 p.

Tuttle, M. L., ms, 1988, Geochemical evolution and depositional history of sediment in modern and ancient saline lakes: Evidence from sulfur geochemistry: Ph.D. thesis, Colorado School of Mines, Golden, Colorado.

Tuttle, M. L., Goldhaber, M. B., and Williamson, D. L., 1986, An analytical scheme for determining forms of sulphur in oil shales and associated rocks: Talanta, v. 33, p. 953–961.

Vaughan, D. J., and Craig, J. R., 1978, Mineral chemistry of metal sulfides: New York, Cambridge University Press, 493 p.

Ward, J. C., 1970, The structure and properties of some iron sulphides: Reviews of Pure and Applied Chemistry, v. 20, p. 175–206.

Zijderveld, J. D. A., 1967, A. C. demagnetization of rocks: Analysis of results, *in* Collinson, D. W., Creer, K. M., and Runcorn, S. K., editors, Methods in palaeomagnetism: Amsterdam, Elsevier, p. 254–286.